Michelson-Morley Experiments: at the crossroads of Relativity, Cosmology and Quantum Physics

Maurizio Consoli

Istituto Nazionale di Fisica Nucleare, Sezione di Catania
Via S.Sofia 64, 95123, Catania, Italy
maurizio.consoli@ct.infn.it

Alessandro Pluchino

Dipartimento di Fisica e Astronomia 'E.Majorana', University of Catania
and Istituto Nazionale di Fisica Nucleare, Sezione di Catania
Via S.Sofia 64, 95123, Catania, Italy
alessandro.pluchino@ct.infn.it

Today, the original Michelson-Morley experiment and its early repetitions at the beginning of the 20th century are considered as a venerable historical chapter for which, at least from a physical point of view, there is nothing more to refine or clarify. The emphasis is now on the modern versions of these experiments, with lasers stabilized by optical cavities, that, apparently, have improved by many orders of magnitude on the limits placed by those original measurements. Though, in those old experiments light was propagating in gaseous systems (air or helium at atmospheric pressure) while now, in modern experiments, light propagates in a high vacuum or inside solid dielectrics. Therefore, in principle, the difference might not depend on the technological progress only but also on the different media that are tested by preventing a straightforward comparison. Starting from this observation, one can formulate a new theoretical scheme where the tiny, irregular residuals observed so far, from Michelson-Morley to the present experiments with optical resonators, point consistently toward the long sought preferred reference frame tight to the CMB. The existence of this scheme, while challenging the traditional 'null interpretation', presented in all textbooks and specialized reviews as a self-evident scientific truth, further emphasizes the central role of these experiments for Relativity, Cosmology and Quantum Physics.

Keywords: Relativity; preferred reference system; quantum nonlocality

arXiv:2402.12421v1 [physics.gen-ph] 19 Feb 2024

2 *Authors' Names*

1. Introduction

From the very beginning there are two interpretations of Relativity: Einstein's Special Relativity[1] and the 'Lorentzian' formulation.[2] Apart from all historical aspects, the difference could simply be phrased as follows. In a Lorentzian approach, the relativistic effects originate from the individual motion of each observer S', S"...with respect to some preferred reference frame Σ, a convenient redefinition of Lorentz' ether. Instead, according to Einstein, eliminating the concept of the ether leads to interpret the same effects as consequences of the *relative* motion of each pair of observers S' and S". This is possible because the basic quantitative ingredients, namely Lorentz Transformations, have a crucial group structure and are the same in both formulations. In the case of one-dimensional motion [a], an intuitive representation is given in Fig.1.
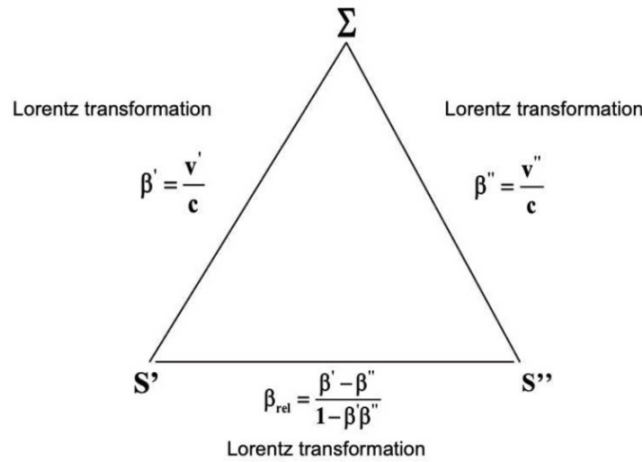

Fig. 1.   *An intuitive representation of the two interpretations of Relativity.*

For this reason, it has been generally assumed that there is a substantial phenomenological equivalence of the two formulations. This point of view was, for instance, already clearly expressed by Ehrenfest in his lecture 'On the crisis of the light ether hypothesis' (Leyden, December 1912) as follows: "So, we see that the ether-less theory of Einstein demands exactly the same here as the ether theory of Lorentz. It is, in fact, because of this circumstance, that according to Einstein's theory an observer must observe exactly the same contractions, changes of rate, etc.

---

[a]We ignore here the subtleties related to the Thomas-Wigner spatial rotation which is introduced when considering two Lorentz transformations along different directions, see e.g.[3–5]

in the measuring rods, clocks, etc. moving with respect to him as in the Lorentzian theory. And let it be said here right away and in all generality. As a matter of principle, there is no experimentum crucis between the two theories". Therefore, by assuming that, in a Lorentzian perspective, the motion with respect to Σ could not be detected, the usual attitude was to consider the difference between the two interpretations as a philosophical problem.

However, it was emphasized by Bell[6] that adopting the Lorentzian point of view could be crucial to reconcile hypothetical faster-than-light signals with causality, as with the apparent non-local aspects of the Quantum Theory. Indeed, if all reference frames are placed on the same footing, as in Special Relativity, how to decide of the time ordering of two events A and B along the world line of a hypothetical effect propagating with speed $> c$? This ordering can be different in different frames, because in some frame S' one could find $t'_A > t'_B$ and in some other frame S'' the opposite $t''_B > t''_A$. This causal paradox, which is the main reason why superluminal signals are not believed to exist, disappears in a Lorentzian formulation where the different views of the two observers become a sort of optical illusion, like an aberration[b].

But the mere logical possibility of Σ is not enough. For a full resolution of the paradox, the $\Sigma-$ frame should show up through a determination of the kinematic parameters β', β''... Thus, we arrive to the main point of this article: the prejudice that, even in a Lorentzian formulation of relativity, the individual β', β''... cannot be experimentally determined. This belief derives from the assumption that the Michelson-Morley type of experiments, from the original 1887 trial to the modern versions with lasers stabilized by optical cavities, give 'null results', namely that the small residuals found in these measurements are just typical instrumental artifacts. We recall that in these precise interferometric experiments, one attempts to detect in laboratory an 'ether-wind', i.e. a small angular dependence of the velocity of light that might indicate the Earth motion with respect to the hypothetical Σ, e.g. the system where the Cosmic Microwave Background (CMB) is isotropic. While in Special Relativity, no ether wind can be observed by definition, in a Lorentzian perspective it is only a 'conspiracy' of relativistic effects which makes undetectable the individual velocity parameters β', β''... But the conspiracy works exactly only when the velocity of light c_γ propagating in the various interferometers coincides with the basic parameter c entering Lorentz transformations. Therefore, one may

---

[b]If S' is connected to Σ by a Lorentz transformation with parameter $\beta' = v'/c$, by the inverse transformation we can find the time coordinates in Σ starting from x'_A, ct'_A, x'_B and ct'_B, namely $cT_A = \gamma'(\beta' x'_A + ct'_A)$ and $cT_B = \gamma'(\beta' x'_B + ct'_B)$, with $1/\gamma' = \sqrt{1 - (\beta')^2}$. Analogously, for S'' and parameter $\beta'' = v''/c$, we will find the same values, i.e. $cT_A = \gamma''(\beta'' x''_A + ct''_A)$ and $cT_B = \gamma''(\beta'' x''_B + ct''_B)$, with now $1/\gamma'' = \sqrt{1 - (\beta'')^2}$. Thus no ambiguity is possible, either $T_A > T_B$ or viceversa so that the view in the preferred $\Sigma-$frame becomes the relevant one to decide on causal effects.

ask, what happens if $c_\gamma \neq c$, for instance when light propagates in air or in gaseous helium as in the old experiments? Starting from this observation, we have formulated a new theoretical scheme[7–10] where the small residuals observed so far, from Michelson-Morley to the present experiments with optical resonators, point consistently toward the long sought preferred reference frame tight to the CMB. In this sense, our scheme is seriously questioning the standard null interpretation of these experiments which is presented in all textbooks and specialized reviews as a self-evident scientific truth. In this article we will review the main results of our extensive work and also propose further experimental tests.

We emphasize that, besides Relativity, our reinterpretation of the data intertwines with and influences other areas of contemporary physics, such as the non-locality of the Quantum Theory, the current vision of the Vacuum State and Cosmology. These implications are so important to deserve a preliminary discussion in this Introduction.

1.1. *Relativity and Quantum Non-Locality*

The existence of intrinsically non-local aspects in the Quantum Theory and the relationship with relativity has been the subject of a countless number of books and articles, growing more and more rapidly in recent times, see e.g.[11–13] for a list of references. The problem dates back to the very early days of Quantum Mechanics, even before the seminal work of Einstein-Podolski-Rosen (EPR).[14] Indeed, the basic issue is already found in Heisenberg's 1929 Chicago Lectures: " We imagine a photon represented by a wave packet... By reflection at a semi-transparent mirror, it is possible to decompose into a reflected and a transmitted packet...After a sufficient time the two parts will be separated by any distance desired; now if by experiment the photon is found, say, in the reflected part of the packet, then the probability of finding the photon in the other part of the packet immediately becomes zero. The experiment at the position of the reflected packet thus exerts a kind of action (reduction of the wave packet) at the distant point and one sees that this action is propagated with a velocity greater than that of light". After that, Heisenberg, almost frightened by his same words, feels the need to add the following remark: "However, it is also obvious that this kind of action can never be utilized for the transmission of signals so that it is not in conflict with the postulates of relativity".

Heisenberg's final observation is one of the first formulations of the so called 'peaceful coexistence'. Actually, presenting as an 'obvious' fact that this type of effects can never be used to communicate between observers at a space-like separation sounds more as a way to avoid the causal paradox, which is present in Special Relativity, when dealing with faster than light signals. But, independently of that, this observation expresses a position that can hardly be considered satisfactory. In fact, if there were really some 'Quantum Information' which propagates with a speed $v_{QI} \gg c$, could such extraordinary thing be so easily dismissed? Namely, could we ignore this 'something' just because, apparently, it cannot be efficiently controlled

to send 'messages'[c]? After all, this explains why Dirac, more than forty years later, was still concluding that "The only theory which we can formulate at the present is a non-local one, and of course one is not satisfied with such a theory. I think one ought to say that the problem of reconciling quantum theory and relativity is not solved".[17]

But only with Bell's contribution[6] the real terms of the problem were fully understood. He clearly spelled out the local, realistic point of view. If physical influences must propagate continuously through space, it becomes unavoidable to complete the quantum formalism by introducing additional 'hidden' variables associated with the space-time regions in question [d]. But, then, it is possible to derive a bound on the degree of correlation of physical systems that are no longer interacting but have interacted in their past. This bound has been used to rule out experimentally[18–20] the class of local, hidden-variable theories which are based on causal influences propagating at subluminal speed. Experimentally excluding this class of theories means rejecting a familiar vision of reality. Thanks to Bell, "A seemingly philosophical debate about the nature of physical reality could be settled by an experiment! ...The conclusion is now clear: Einstein's view of physical reality cannot be upheld".[21]

Thus, the importance of Bell's work cannot be underestimated: "Bell's result combined with the EPR argument was not a 'no hidden variables theorem' but a non-locality theorem, the impossibility of hidden variables being only one step in a two-step argument...It means that some action at a distance exists in Nature, even though it does not say what this action consists of".[13] It was this awareness to give him the perception that "... we have an apparent incompatibility, at the deepest level, between the two fundamental pillars of contemporary theory",[6] namely Quantum Theory and Special Relativity. This inspired his view where the existence of the preferred $\Sigma-$frame would free ourselves from the no-signalling argument to dispose of the causality paradox.

---

[c]Experimental correlations between spacelike separated measurements can in principle be explained through hidden influences propagating at a finite speed $v_{\rm QI} \gg c$ provided $v_{\rm QI}$ is large enough.[15] But in ref.[16] it is also shown that for any finite $v_{\rm QI}$, with $c < v_{\rm QI} < \infty$, one can construct combined correlations to be used for faster-than-light communication.

[d] "In particular, Jordan had been wrong in supposing that nothing was real or fixed in the microscopic world before observation. For after observing only one of the two particles the result of subsequently observing the other (possibly at very remote place) is immediately predictable. Could it be that the first measurement somehow fixes what was unfixed or makes real what was unreal, not only for the near particle but also for the remote one? For EPR that would be an unthinkable 'spooky action at distance'. To avoid such action at distance one has to attribute, to the space-time regions in question, real correlated properties in advance of the observation which predetermine the outcome of these particular observations. Since these real properties, fixed in advance of the observation, are not contained in the quantum formalism, that formalism for EPR is incomplete".[6]

1.2. *Relativity and the Vacuum State*

A frequent objection to the idea of relativity with a preferred frame is that, after all, Quantum Mechanics is not a fundamental description of the world. What about, if we started from a more fundamental Quantum Field Theory (QFT)? In this perspective, the issue of the preferred frame can be reduced to find a particular, logical step that prevents to deduce that Einstein Special Relativity, with no preferred frame, is the *physically realized* version of relativity. This is the version which is always assumed when computing S-matrix elements for microscopic processes. However, what one is actually using is the machinery of Lorentz transformations whose first, complete derivation dates back, ironically, to Larmor and Lorentz who were assuming the existence of a fundamental state of rest (the ether).

Our point, discussed in,[22–25] is that there is indeed a particular element which has been missed so far and which concerns the assumed Lorentz invariance of the vacuum state. Even though one is still using the Latin word 'vacuum', which means empty, here we are dealing with the lowest energy state. According to the present view, this is not trivially empty but is determined by the condensation process of some elementary quanta [e]. Namely the energy is minimized when these quanta, such as Higgs particles, quark-antiquark pairs, gluons... macroscopically occupy the same quantum state, i.e. the zero-3-momentum state [f]. Thus, if the condensation process singles out a certain reference frame Σ, the fundamental question is how to reconcile this picture with the basic postulate of axiomatic QFT: the exact Lorentz invariance of the vacuum.[28] This postulate, meaning that the vacuum state must remain unchanged under Lorentz boost, should not be confused with the condition that only local scalars (as the Higgs field, or the gluon condensate, or the chiral condensate...) acquire a non-zero vacuum expectation value.

To make this evident, let us introduce the reference vacuum state $|\Psi^{(0)}\rangle$, appropriate to the observer at rest in the $\Sigma-$frame singled out by the condensation process, and the corresponding vacuum states $|\Psi'\rangle$, $|\Psi''\rangle$,... appropriate to moving observers S', S'',... By assuming that these different vacua are generated by

---

[e]Before our work, the idea that the phenomenon of vacuum condensation could produce 'conceptual tensions' with both Special and General Relativity, was discussed by Chiao:[26] "The physical vacuum, an intrinsically nonlocal ground state of a relativistic quantum field theory, which possesses certain similarities to the ground state of a superconductor... This would produce an unusual 'quantum rigidity' of the system, associated with what London called the 'rigidity of the macroscopic wave function'... The Meissner effect is closely analog to the Higgs mechanism in which the physical vacuum also spontaneously breaks local gauge invariance ".[26]

[f]In the physically relevant case of the Standard Model, the phenomenon of vacuum condensation can be summarized by saying that "What we experience as empty space is nothing but the configuration of the Higgs field that has the lowest possible energy. If we move from field jargon to particle jargon, this means that empty space is actually filled with Higgs particles. They have Bose condensed".[27]

Lorentz boost unitary operators U', U''...acting on $|\Psi^{(0)}\rangle$, say $|\Psi'\rangle = U'|\Psi^{(0)}\rangle$, $|\Psi''\rangle = U''|\Psi^{(0)}\rangle$... For any Lorentz-scalar operator G, such that $G = (U')^\dagger G U' = (U'')^\dagger G U''$..., it follows trivially

$$\langle G \rangle_{\Psi^{(0)}} = \langle G \rangle_{\Psi'} = \langle G \rangle_{\Psi''} = .. \tag{1}$$

However, this by no means implies $|\Psi^{(0)}\rangle = |\Psi'\rangle = |\Psi''\rangle$... To this end, one should construct explicitly the three boost generators L_{0i} (with i=1,2,3) and show that $L_{0i}|\Psi^{(0)}\rangle = 0$. But, in four space-time dimensions, the explicit construction of these operators, and of the corresponding Poincaré algebra [g] is only known for the free-field case through the simple Wick-ordering prescription relatively to the free-field vacuum $|0\rangle$. In an interacting theory, the construction is implemented order by order in perturbation theory. Therefore, in the presence of non-perturbative phenomena (such as Spontaneous Symmetry Breaking, chiral symmetry breaking, gluon condensation...) where the physical vacuum $|\Psi^{(0)}\rangle$ cannot be constructed from the free-field vacuum $|0\rangle$ order by order in perturbation theory, proving the Lorentz invariance of the vacuum represents an insurmountable problem. In this situation, with a Lorentz-invariant interaction, the resulting theory will still be Lorentz covariant but, with a non-Lorentz-invariant vacuum, there would be a preferred reference frame [h].

1.3. *Relativity and the CMB*

Finally, some remarks about the physical nature of the hypothetical $\Sigma-$frame. A natural candidate is the reference system where the temperature of the CMB looks exactly isotropic or, more precisely, where the CMB kinematic dipole[30] vanishes. This dipole is in fact a direct consequence of the motion of the Earth ($\beta = V/c$)

$$T(\theta) = \frac{T_o\sqrt{1 - \beta^2}}{1 - \beta\cos\theta} \tag{2}$$

---

[g]This means an operatorial representation of the 10 generators P_μ and $L_{\mu\nu}$ (μ, ν= 0, 1, 2, 3), where P_μ describe the space-time translations and $L_{\mu\nu} = -L_{\nu\mu}$ the space rotations and Lorentz boosts, with commutation relations $[P_\mu, P_\nu] = 0$, $[L_{\mu\nu}, P_\rho] = i\eta_{\nu\rho}P_\mu - i\eta_{\mu\rho}P_\nu$ and $[L_{\mu\nu}, L_{\rho\sigma}] = -i\eta_{\mu\rho}L_{\nu\sigma} + i\eta_{\mu\sigma}L_{\nu\rho} - i\eta_{\nu\sigma}L_{\mu\rho} + i\eta_{\nu\rho}L_{\mu\sigma}$ where $\eta_{\mu\nu} = \text{diag}(1,-1,-1,-1)$ is the Minkowski tensor. A Lorentz-invariant vacuum has to be annihilated by all 10 generators.

[h]To our knowledge,in four space-time dimensions, a non-perturbative analysis of a Lorentz-invariant vacuum has been attempted by very few authors. In the case of non-linear field theories with $P(\Phi(x))$ interactions, such as $\Phi^4(x)$, this was discussed by Segal.[29] He considered a suitable generalization of the standard Wick ordering : $P(\Phi)$: relative to $|0\rangle$, say :: $P(\Phi)$ ::, such that $\langle\Psi^{(0)}| :: P(\Phi) :: |\Psi^{(0)}\rangle = 0$ in the true vacuum state. His conclusion was that :: $P(\Phi)$ :: is not well-defined until the physical vacuum is known, but, at the same time, the physical vacuum also depends on the definition given for :: $P(\Phi)$ ::. From this type of circularity Segal concluded that, in general, in such a nonlinear QFT, the physical vacuum will *not* be invariant under the full Lorentz symmetry of the underlying Lagrangian density.

Accurate observations with satellites in space[31] have shown that the measured temperature variations correspond to a motion of the solar system described by an average velocity $V \sim 370$ km/s, a right ascension $\alpha \sim 168^o$ and a declination $\gamma \sim -7^o$, pointing approximately in the direction of the Leo constellation. This means that, if one sets $T_o \sim 2.7$ K and $\beta \sim 0.00123$, there are angular variations of a few millikelvin

$$\Delta T^{\text{CMB}}(\theta) \sim T_o\beta\cos\theta = \pm 3.3 \text{ mK} \tag{3}$$

which represent by far the dominant contribution to the CMB anisotropy.

Could the reference system with vanishing CMB dipole represent the fundamental preferred frame for relativity as in the original Lorentzian formulation? The standard answer is that one should not confuse these two concepts. The CMB is a definite medium and, as such, sets a rest frame where the dipole anisotropy is zero. Our motion with respect to this system has been detected but, by itself, this is not in contradiction with Special Relativity. Though, to good approximation, this kinematic dipole arises by combining the various forms of peculiar motion which are involved (rotation of the solar system around the center of the Milky Way, motion of the Milky Way toward the center of the Local Group, motion of the Local Group of galaxies in the direction of the Great Attractor...)[31] . Thus, if one could switch-off the local inhomogeneities that produce these peculiar forms of motion, it is natural to imagine a global frame of rest associated with the Universe as a whole. A vanishing CMB dipole could then just *indicate* the existence of this fundamental system Σ that we may conventionally decide to call 'ether' but the cosmic radiation itself would not *coincide* with this form of ether.

This is why, to discriminate between the two concepts, Michelson-Morley type of experiments become crucial. Detecting a small angular dependence of the velocity of light in the Earth laboratory, and correlating this angular dependence with the Earth cosmic motion, would provide the missing link with the logical arguments from Quantum Non-Locality [i] and with the idea of a condensed vacuum which selects a particular reference frame through the macroscopic occupation of the same zero 3-momentum state. More generally a non-null interpretation of the Michelson-Morley experiments would resolve the puzzle of a world endowed with a fundamental space and a fundamental time whose existence, otherwise, would remain forever hidden to us.

After this general Introduction, we will start by reviewing in Sect.2 the basic ingredients for a modern analysis of the Michelson-Morley experiments. Then we will summarize in Sects.3 and 4 our re-analysis[7–10] of the classical experiments

---

[i] "Non-Locality is most naturally incorporated into a theory in which there is a special frame of reference. One possible candidate for this special frame of reference is the one in which the CMB is isotropic. However, other than the fact that a realistic interpretation of quantum mechanics requires a preferred frame and the CMB provides us with one, there is no readily apparent reason why the two should be linked".[32]

and in Sect.5 the corresponding treatment of the present experiments with optical resonators. As a matter of fact, once the small residuals are analyzed in our scheme, the long sought $\Sigma-$frame tight to the CMB is naturally emerging. Sect.6 will finally contain a summary and our conclusions.

2. A modern view of the 'ether-drift' experiments

The Michelson-Morley experiments are also called 'ether-drift' experiments because they were designed to detect the drift of the Earth in the ether by observing a dragging of light associated with the Earth cosmic motion. Today, experimental evidence for both the undulatory and corpuscular aspects of radiation has substantially modified the consideration of an underlying ethereal medium, as support of the electromagnetic waves, and its logical need for the physical theory. Besides, Lorentz Transformations forbid dragging and the irregular behavior of the small observed residuals is inconsistent with the smooth time modulations that one would expect from the Earth rotation. Therefore, at first sight, the idea of detecting a non-null effect seems hopeless.

However, as anticipated, dragging is only forbidden if the velocity of light in the interferometers is the same parameter c of Lorentz transformations. For instance, when light propagates in a gas, the sought effect of a preferred system Σ could be due to the small fraction of refracted light. Obviously, this would be much smaller than classically expected but, in view of the extraordinary precision of the interferometers, it could still be measurable. In addition, the idea of smooth time modulations of the signal reflects the traditional identification of the local velocity field, which describes the drift, with the projection of the global Earth motion at the experimental site. This identification is equivalent to a form of regular, laminar flow where global and local velocity fields coincide. Instead, depending on the nature of the physical vacuum, the two velocity fields could only be related indirectly, as it happens in turbulent flows, so that numerical simulations would be needed for a consistent statistical description of the data.

In the following, we will summarize the scheme of refs.[7–10] starting with the case of light propagating in gaseous media, as for the classical experiments.

2.1. *Basics of the ether-drift experiments*

In the classical measurements in gases (Michelson-Morley, Miller, Tomaschek, Kennedy, Illingworth, Piccard-Stahel, Michelson-Pease-Pearson, Joos)[33]-,[43] one was measuring the fringe shifts produced by a rotation of the interferometer. Instead, in modern experiments, with lasers stabilized by optical cavities, see e.g.[44] for a review, one measures frequency shifts. The modern experiments adopt a different technology but, in the end, have exactly the same scope: searching for an anisotropy of the two-way velocity of light $\bar{c}_\gamma(\theta)$ which is the only one that can be measured
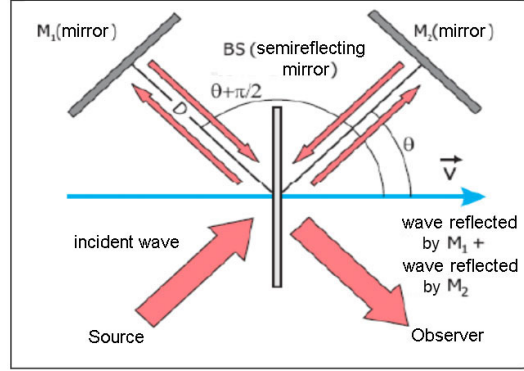
Fig. 2.   *A schematic illustration of the Michelson interferometer. Note that, by computing the transit times as in Eq.(6), we are assuming the validity of Lorentz transformations so that the length of a rod does not depend on its orientation in the frame S where it is at rest.*

unambiguously

$$\bar{c}_\gamma(\theta) = \frac{2c_\gamma(\theta)c_\gamma(\pi+\theta)}{c_\gamma(\theta) + c_\gamma(\pi+\theta)} \tag{4}$$

By introducing its anisotropy

$$\Delta\bar{c}_\theta = \bar{c}_\gamma(\pi/2+\theta) - \bar{c}_\gamma(\theta) \tag{5}$$

there is a simple relation with the time difference $\Delta t(\theta)$ for light propagation back and forth along perpendicular rods of length D. In fact, by assuming the validity of Lorentz transformations, the length of a rod does not depend on its orientation, in the S frame where it is at rest, see Fig.2, and one finds,

$$\Delta t(\theta) = \frac{2D}{\bar{c}_\gamma(\theta)} - \frac{2D}{\bar{c}_\gamma(\pi/2+\theta)} \sim \frac{2D}{c}\ \frac{\Delta\bar{c}_\theta}{c} \tag{6}$$

(where, in the last relation, we have assumed that light propagates in a medium of refractive index $\mathcal{N} = 1 + \epsilon$, with $\epsilon \ll 1$). This gives directly the fringe patterns (λ is the light wavelength)

$$\frac{\Delta\lambda(\theta)}{\lambda} \sim \frac{2D}{\lambda}\ \frac{\Delta\bar{c}_\theta}{c} \tag{7}$$

which were measured in the classical experiments.

    In modern experiments, on the other hand, a possible anisotropy of $\bar{c}_\gamma(\theta)$ would show up through the relative frequency shift, i.e. the beat signal, $\Delta\nu(\theta)$ of two orthogonal optical resonators, see Fig.3. Their frequency

$$\nu(\theta) = \frac{\bar{c}_\gamma(\theta)m}{2L} \tag{8}$$

is proportional to the two-way velocity of light within the resonator through an integer number m, which fixes the cavity mode, and the length of the cavity L as
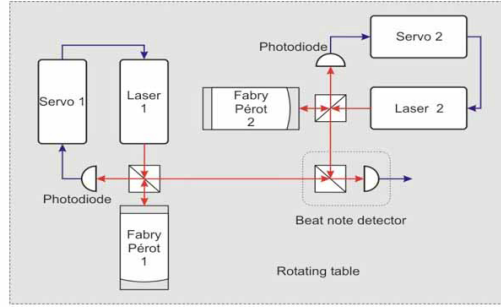
Fig. 3.   *The scheme of a modern ether-drift experiment. The light frequencies are first stabilized by coupling the lasers to Fabry-Perot optical resonators. The frequencies ν_1 and ν_2 of the resonators are then compared in the beat note detector which provides the frequency shift $\Delta\nu(\theta) = \nu_1(\pi/2 + \theta) - \nu_2(\theta)$. For a review, see e.g.*[44]

measured in the laboratory S' frame. Therefore, once the length of a cavity in its rest frame does not depend on its orientation, one finds

$$\frac{\Delta\nu(\theta)}{\nu_0} \sim \frac{\Delta\bar{c}_\theta}{c} \qquad (9)$$

where ν_0 is the reference frequency of the two resonators.

2.2. *The limit of refractive index $\mathcal{N} = 1 + \epsilon$*

Let us consider light propagating in a medium which is close to the ideal vacuum limit, i.e. whose refractive index is $\mathcal{N} = 1 + \epsilon$ with $\epsilon \ll 1$. The medium (e.g. a gas) fills an optical cavity at rest in a frame S which moves with velocity v with respect to the hypothetical Σ. Now, by assuming i) that the velocity of light is exactly isotropic when $S \equiv \Sigma$ and ii) the validity of Lorentz transformations, then any anisotropy in S should vanish identically either for $v = 0$ or for the ideal vacuum case $\mathcal{N} = 1$ when the velocity of light c_γ coincides with the basic parameter c of Lorentz transformations. Thus, one can expand in powers of the two small parameters ϵ and $\beta = v/c$. By taking into account that, by its very definition, the two-way velocity $\bar{c}_\gamma(\theta)$ is invariant under the replacement $\beta \to -\beta$ and that, for any fixed β, is also invariant under the replacement $\theta \to \pi + \theta$, to lowest non-trivial level $\mathcal{O}(\epsilon\beta^2)$, one finds the general expression[7, 24]

$$\bar{c}_\gamma(\theta) \sim \frac{c}{\mathcal{N}}\left[1 - \epsilon\,\beta^2 \sum_{n=0}^{\infty} \zeta_{2n} P_{2n}(\cos\theta)\right] \qquad (10)$$

Here, to take into account invariance under $\theta \to \pi + \theta$, the angular dependence has been given as an infinite expansion of even-order Legendre polynomials with arbitrary coefficients $\zeta_{2n} = \mathcal{O}(1)$. In Einstein's Special Relativity, where there is

no preferred reference frame, these ζ_{2n} coefficients should vanish identically. In a Lorentzian approach, on the other hand, there is no reason why they should vanish *a priori* [j].

By leaving out the first few ζ's as free parameters in the fits, Eq.(10) could already represent a viable form to compare with experiments. Still, one can further sharpen the predictions by exploiting one more derivation of the $\epsilon \to 0$ limit with a preferred frame. This other argument is based on the effective space-time metric $g^{\mu\nu} = g^{\mu\nu}(\mathcal{N})$ which, through the relation $g^{\mu\nu}p_\mu p_\nu = 0$, describes light propagation in a medium of refractive index $\mathcal{N}$. For the quantum theory, a derivation of this metric from first principles was given by Jauch and Watson[46] who worked out the quantization of the electromagnetic field in a dielectric. They noticed that the procedure introduces unavoidably a preferred reference frame, the one where the photon energy spectrum does not depend on the direction of propagation, and which is "usually taken as the system for which the medium is at rest". However, such an identification reflects the point of view of Special Relativity with no preferred frame. Instead, one can adapt their results to the case where the angle-independence of the photon energy is only valid when both medium and observer are at rest in some particular frame Σ.

In this perspective, let us consider two identical optical cavities, namely cavity 1, at rest in Σ, and cavity 2, at rest in S, and denote by $\pi_\mu \equiv (\frac{E_\pi}{c}, \pi)$ the light 4-momentum for Σ in his cavity 1 and by $p_\mu \equiv (\frac{E_p}{c}, \mathbf{p})$ the corresponding light 4-momentum for S in his cavity 2. Let us also denote by $g^{\mu\nu}$ the space-time metric that S uses in the relation $g^{\mu\nu}p_\mu p_\nu = 0$ and by

$$\gamma^{\mu\nu} = \text{diag}(\mathcal{N}^2, -1, -1, -1) \tag{11}$$

the metric used by Σ in the relation $\gamma^{\mu\nu}\pi_\mu\pi_\nu = 0$ and which gives an isotropic velocity $c_\gamma = E_\pi/|\pi| = \frac{c}{\mathcal{N}}$.

Now, Special Relativity was formulated, more than a century ago, by assuming the perfect equivalence of two reference systems in uniform translational motion. Instead, with a preferred frame Σ, as far as light propagation is concerned, this physical equivalence is only assumed in the ideal $\mathcal{N} = 1$ limit. As anticipated, for $\mathcal{N} \neq 1$, where light gets absorbed and then re-emitted, the fraction of refracted light could keep track of the particular motion of matter with respect to Σ and produce, in the frame S where matter is at rest, an angular dependence of the velocity of light. Equivalently, assuming that the solid parts of cavity 2 are at rest in a frame S, which is in uniform translational motion with respect to Σ, no longer implies that the medium which stays inside, e.g. the gas, is in a state of thermodynamic

---

[j]As anticipated, for Lorentz, only a conspiracy of effects prevents to detect the motion with respect to the ether, which, however different might be from ordinary matter, is nevertheless endowed with a certain degree of substantiality. For this reason, in his view, "it seems natural not to assume at starting that it can never make any difference whether a body moves through the ether or not".[45]

equilibrium[k]. Thus, one should keep an open mind and exploit the implications of the basic condition

$$g^{\mu\nu}(\mathcal{N}=1) = \gamma^{\mu\nu}(\mathcal{N}=1) = \eta^{\mu\nu} \tag{12}$$

where $\eta^{\mu\nu}$ is the Minkowski tensor. This standard equality amounts to introduce a transformation matrix, say A^μ_ν, such that

$$g^{\mu\nu} = A^\mu_\rho A^\nu_\sigma \eta^{\rho\sigma} = \eta^{\mu\nu} \tag{13}$$

This relation is strictly valid for $\mathcal{N}=1$. However, by continuity, one is driven to conclude that an analogous relation between $g^{\mu\nu}$ and $\gamma^{\mu\nu}$ should also hold in the $\epsilon \to 0$ limit. The only subtlety is that relation (13) does not fix uniquely A^μ_ν. In fact, one can either choose the identity matrix, i.e. $A^\mu_\nu = \delta^\mu_\nu$, or a Lorentz transformation, i.e. $A^\mu_\nu = \Lambda^\mu_\nu$. Since for any finite v these two matrices cannot be related by an infinitesimal transformation, it follows that A^μ_ν is a two-valued function in the $\epsilon \to 0$ limit. Therefore, in principle, there are two solutions. If A^μ_ν is the identity matrix, we find a first solution

$$[g^{\mu\nu}(\mathcal{N})]_1 = \gamma^{\mu\nu} \sim \eta^{\mu\nu} + 2\epsilon\delta^\mu_0\delta^\nu_0 \tag{14}$$

while, if A^μ_ν is a Lorentz transformation, we find the other solution

$$[g^{\mu\nu}(\mathcal{N})]_2 = \Lambda^\mu_\rho \Lambda^\nu_\sigma \gamma^{\rho\sigma} \sim \eta^{\mu\nu} + 2\epsilon v^\mu v^\nu \tag{15}$$

v^μ being the dimensionless S 4-velocity, $v^\mu \equiv (v^0, \mathbf{v}/c)$ with $v_\mu v^\mu = 1$.

Notice that with the former choice, implicitly adopted in Special Relativity to preserve isotropy in all reference systems also for $\mathcal{N} \neq 1$, one is introducing a discontinuity in the transformation matrix for any $\epsilon \neq 0$. Indeed, the whole emphasis on Lorentz transformations depends on enforcing Eq.(13) for $A^\mu_\nu = \Lambda^\mu_\nu$ so that $\Lambda^{\mu\sigma}\Lambda^\nu_\sigma = \eta^{\mu\nu}$ and the Minkowski metric applies to all equivalent frames.

On the other hand, with the latter solution, by replacing in the relation $p_\mu p_\nu g^{\mu\nu} = 0$, the photon energy now depends on the direction of propagation. Then, by defining the light velocity $c_\gamma(\theta)$ from the ratio $E_p/|\mathbf{p}|$, one finds[7,24]

$$c_\gamma(\theta) \sim \frac{c}{\mathcal{N}} \left[1 - 2\epsilon\beta\cos\theta - \epsilon\beta^2(1+\cos^2\theta)\right] \tag{16}$$

and a two-way velocity

$$\bar{c}_\gamma(\theta) = \frac{2c_\gamma(\theta)c_\gamma(\pi+\theta)}{c_\gamma(\theta)+c_\gamma(\pi+\theta)} \sim \frac{c}{\mathcal{N}} \left[1 - \epsilon\beta^2\left(1+\cos^2\theta\right)\right] \equiv \frac{c}{\bar{\mathcal{N}}(\theta)} \tag{17}$$

---

[k]Think for instance of the collective interaction of a gaseous medium with the CMB radiation or with hypothetical dark matter in the Galaxy. However weak this interaction may be, it would mimic a non-local thermal gradient that could bring the gas out of equilibrium. The advantage of the following analysis is that it only uses symmetry properties without requiring a knowledge of the underlying dynamical processes.

14   *Authors' Names*

here θ is the angle between $\mathbf{v}$ and $\mathbf{p}$ (as defined in the S frame) and

$$\bar{\mathcal{N}}(\theta) \sim \mathcal{N} \left[1 + \epsilon \beta^2 (1 + \cos^2 \theta)\right] \tag{18}$$

Eq.(17) corresponds to setting in Eq.(10) $\zeta_0 = 4/3$, $\zeta_2 = 2/3$ and all $\zeta_{2n} = 0$ for $n > 1$ and can be considered a modern version of Maxwell's original calculation.[48] It represents a definite, alternative model for the interpretation of experiments performed close to the ideal vacuum limit $\epsilon = 0$, such as in gaseous systems, and will be adopted in the following [1].

3. A first look at the classical experiments

From Eq.(17) we find a fractional anisotropy

$$\frac{\Delta \bar{c}_\theta}{c} = \frac{\bar{c}_\gamma(\pi/2 + \theta) - \bar{c}_\gamma(\theta)}{c} \sim \epsilon \, (v^2/c^2) \cos 2\theta \tag{19}$$

which produces a fringe pattern

$$\frac{\Delta \lambda(\theta)}{\lambda} = \frac{2D}{\lambda} \, \frac{\Delta \bar{c}_\theta}{c} \sim \frac{D}{\lambda} \, 2\epsilon \, \frac{v^2}{c^2} \cos 2\theta \tag{20}$$

The dragging of light in the Earth frame is then described as a pure 2nd-harmonic effect, which is periodic in the range $[0, \pi]$, as in the classical theory (see e.g.[47]). However, its amplitude

$$A_2 = \frac{D}{\lambda} \, 2\epsilon \, \frac{v^2}{c^2} \tag{21}$$

is now much smaller being suppressed by the factor 2ϵ relatively to the classical value. This was traditionally reported for the orbital velocity of 30 km/s as

$$A_2^{\text{class}} = \frac{D}{\lambda} \left(\frac{30 \text{ km/s}}{c}\right)^2 \tag{22}$$

This difference could then be re-absorbed into an *observable* velocity which is related to the *kinematical* velocity v through the gas refractive index

$$v_{\text{obs}}^2 \sim 2\epsilon v^2 \tag{23}$$

so that

$$A_2 = \frac{D}{\lambda} \, \frac{v_{\text{obs}}^2}{c^2} \tag{24}$$

---

[1]A conceptual detail concerns the relation of the gas refractive index $\mathcal{N}$, as defined in the $\Sigma-$frame through Eq.(11), to the experimental quantity $\mathcal{N}_{\text{exp}}$ which is extracted from measurements of the two-way velocity in the Earth laboratory. By assuming a $\theta-$dependent refractive index as in Eq.(18) one should thus define $\mathcal{N}_{\text{exp}}$ by an angular average, i.e. $\mathcal{N}_{\text{exp}} \equiv \langle \bar{\mathcal{N}}(\theta) \rangle_\theta = \mathcal{N} \left[1 + \frac{3}{2}(\mathcal{N} - 1)\beta^2\right]$. One can then determine the unknown value $\mathcal{N} \equiv \mathcal{N}(\Sigma)$ (as if the container of the gas were at rest in Σ), in terms of the experimentally known quantity $\mathcal{N}_{\text{exp}} \equiv \mathcal{N}(\text{Earth})$ and of v. As discussed in refs.[7]-,[10] for $v \sim 370$ km/s, the resulting difference $|\mathcal{N}_{\text{exp}} - \mathcal{N}| \lesssim 10^{-9}$ is well below the experimental accuracy on $\mathcal{N}_{\text{exp}}$ and, for all practical purposes, can be ignored.
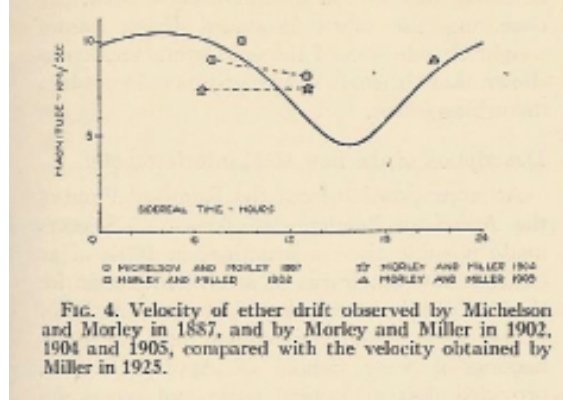
FIG. 4. Velocity of ether drift observed by Michelson and Morley in 1887, and by Morley and Miller in 1902, 1904 and 1905, compared with the velocity obtained by Miller in 1925.

Fig. 4.   *The observable velocity reported by Miller[35] for various experiments.*

Thus, this $v_{\rm obs}$ is the small velocity traditionally extracted from the measured amplitude $A_2^{\rm EXP}$ in the classical analysis of the experiments

$$v_{\rm obs} \sim 30 \text{ km/s } \sqrt{\frac{A_2^{\rm EXP}}{A_2^{\rm class}}} \qquad (25)$$

see e.g. Fig.4.

We can now understand the pattern observed in the classical experiments. For instance, in the original Michelson-Morley experiment, where $\frac{D}{\lambda} \sim 2 \cdot 10^7$, the classically expected amplitude was $A_2^{\rm class} \sim 0.2$. But the experimental amplitude measured in the six sessions was $A_2^{\rm EXP} = 0.01 \div 0.02$. This corresponds to an average anisotropy $\frac{|\Delta \bar{c}_\theta|_{\rm exp}}{c} \sim 4 \cdot 10^{-10}$ and was originally interpreted in terms of a velocity $v_{\rm obs} \sim 8$ km/s. However, for an experiment in air at room temperature and atmospheric pressure where $\epsilon \sim 2.8 \cdot 10^{-4}$, this observable velocity would now correspond to a true kinematic value $v \sim 340$ km/s which would fit well with the cosmic motion indicated by the CMB dipole anistropy. Therefore, the importance of the issue requires to sharpen the analysis of the old experiments, starting from the early 1887 trials.

3.1. *The 1887 Michelson-Morley experiment in Cleveland*

The precision of the Michelson-Morley apparatus[33] was extraordinary, about ± 0.004 of a fringe. For all details, we address the reader to our book.[9] Here, we just limit ourselves to quote from Born.[49] When discussing the classically expected fringe shift upon rotation of the apparatus by 90 degrees, namely $2A_2^{\rm class} \sim 0.4$, he says explicitly: "Michelson was certain that the one-hundredth part of this displacement would still be observable" (i.e. 0.004). As a check, the Michelson-Morley fringe shifts were recomputed in refs.[7,9,50] from the original article,[33] see Table 1. These data

were then analyzed in a Fourier expansion, see e.g. Fig.5 (note that a 1st-harmonic has to be present in the data due to the arrangement of the mirrors needed to have fringes of finite width, see[35, 51]). One can thus extract amplitude and phase of the 2nd-harmonic component by fitting the even combination of fringe shifts

$$B(\theta) = \frac{\Delta\lambda(\theta) + \Delta\lambda(\pi + \theta)}{2\lambda} \qquad (26)$$

see Fig.6.

Table 1.   The fringe shifts $\frac{\Delta\lambda(i)}{\lambda}$ for all noon (n.) and evening (e.) sessions of the Michelson-Morley experiment. The angle of rotation is defined as $\theta = \frac{i-1}{16}\, 2\pi$. The Table is taken from ref.[7]

i	July 8 (n.)	July 9 (n.)	July 11 (n.)	July 8 (e.)	July 9 (e.)	July 12 (e.)
1	−0.001	+0.018	+0.016	−0.016	+0.007	+0.036
2	+0.024	−0.004	−0.034	+0.008	−0.015	+0.044
3	+0.053	−0.004	−0.038	−0.010	+0.006	+0.047
4	+0.015	−0.003	−0.066	+0.070	+0.004	+0.027
5	−0.036	−0.031	−0.042	+0.041	+0.027	−0.002
6	−0.007	−0.020	−0.014	+0.055	+0.015	−0.012
7	+0.024	−0.025	+0.000	+0.057	−0.022	+0.007
8	+0.026	−0.021	+0.028	+0.029	−0.036	−0.011
9	−0.021	−0.049	+0.002	−0.005	−0.033	−0.028
10	−0.022	−0.032	−0.010	+0.023	+0.001	−0.064
11	−0.031	+0.001	−0.004	+0.005	−0.008	−0.091
12	−0.005	+0.012	+0.012	−0.030	−0.014	−0.057
13	−0.024	+0.041	+0.048	−0.034	−0.007	−0.038
14	−0.017	+0.042	+0.054	−0.052	+0.015	+0.040
15	−0.002	+0.070	+0.038	−0.084	+0.026	+0.059
16	+0.022	−0.005	+0.006	−0.062	+0.024	+0.043

The 2nd-harmonic amplitudes for the six experimental sessions are reported in Table 2. Due to their statistical consistency, one can compute the mean and variance and obtain $A_2^{\mathrm{EXP}} \sim 0.016 \pm 0.006$. This value is consistent with an observable velocity

$$v_{\mathrm{obs}} \sim 8.5\; {}^{+1.7}_{-2.2} \quad \mathrm{km/s} \qquad (27)$$

in complete agreement with Miller, ses Fig.4. In this sense, our re-analysis supports the claims of Hicks and Miller. The fringe shifts were much smaller than expected but in two experimental sessions (11 July noon and 12 July evening), the second-harmonic amplitude is non-zero at the 5σ level and in other two sessions (July 9 noon and July 8 evening) is non-zero at the 3σ level. As such, the average measured amplitude $A_2^{\mathrm{EXP}} \sim 0.016$, although much smaller than the classical expectation $A_2^{\mathrm{class}} \sim 0.2$, was not completely negligible. Thus it is natural to ask: should this
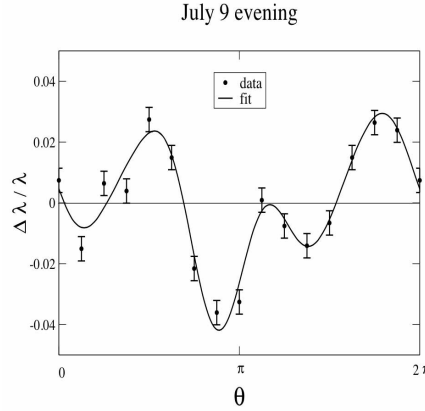
July 9 evening

Fig. 5.   *The fringe shifts for the session of July 9 evening. The fit is performed by including terms up to fourth harmonics. The figure is taken from ref.[50]*
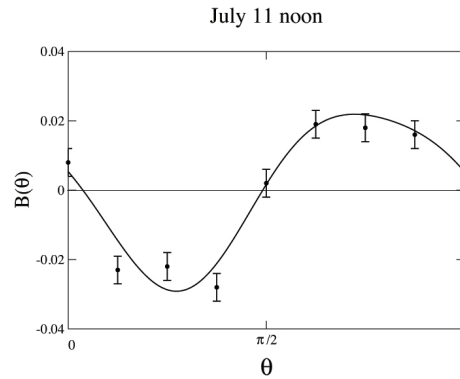
July 11 noon

Fig. 6.   *A fit to the even combination $B(\theta)$ Eq.(26). The second harmonic amplitude is $A_2^{\mathrm{EXP}} = 0.025 \pm 0.005$ and the fourth harmonic is $A_4^{\mathrm{EXP}} = 0.004 \pm 0.005$. The figure is taken from ref.[50]*

value be interpreted as a typical instrumental artifact (a "null result") or could also indicate a genuine ether-drift effect? Of course, this question is not new and, in the past, greatest experts have raised objections to the standard null interpretation of the data. This point of view was well summarized by Miller in 1933[35] as follows: "The brief series of observations (by Michelson and Morley) was sufficient to show clearly that the effect did not have the anticipated magnitude. However, and this fact must be emphasized, *the indicated effect was not zero*". The same conclusion had already been obtained by Hicks in 1902:[51] "The data published by Michelson and Morley, instead of giving a null result, show distinct evidence for an effect of the kind to be expected". There was a 2nd-harmonic effect whose amplitude, however, was substantially smaller than the classical expectation (see Fig.7).

Thus the real point about the Michelson-Morley data does *not* concern the small

Table 2.   The 2nd-harmonic amplitudes for the six experimental sessions of the Michelson-Morley experiment. The table is taken from ref.[7]

SESSION	A_2^{EXP}
July 8 (noon)	0.010 ± 0.005
July 9 (noon)	0.015 ± 0.005
July 11 (noon)	0.025 ± 0.005
July 8 (evening)	0.014 ± 0.005
July 9 (evening)	0.011 ± 0.005
July 12 (evening)	0.024 ± 0.005
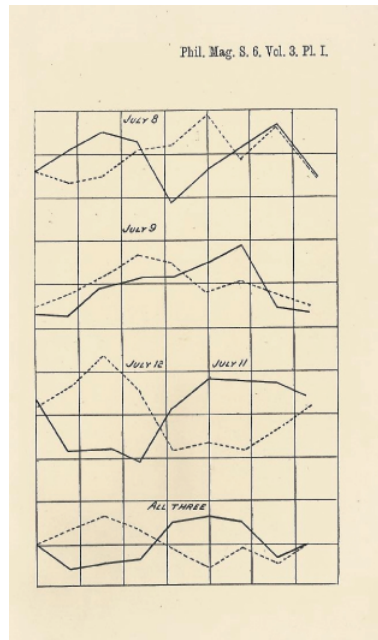
Fig. 7.   *The even combination of fringe shifts $B(\theta)$ for the Michelson-Morley data as reported by Hicks.[51] Solid and dashed lines refer respectively to noon and evening observations. Compare the solid curve of July 11th with the analogous curve in Fig.6.*

magnitude of the amplitude but the sizeable changes in the 'azimuth', i.e in the phase θ_2 of the 2nd-harmonic which gives the direction of the drift in the plane of the interferometer. By performing observations at the same hour on consecutive days (so that variations in the orbital motion are negligible) one expects that this angle should remain the same within the statistical errors. Now, by taking into

account that, in a 2nd-harmonic effect, the angle is always defined up to $\pm 180^o$, one choice for the experimental θ_2-values is $357^o \pm 14^o$, $285^o \pm 10^o$ and $317^o \pm 8^o$ respectively for the noon sessions of July 8th, 9th and 11th. For this assignment, the individual velocity vectors $v_{\rm obs}(\cos\theta_2, -\sin\theta_2)$ and their mean are shown in Fig. 8. As a consequence, directly averaging the amplitudes of the individual sessions is considerably different from first performing the vector average of the data and then computing the resulting amplitude. In the latter case, the average amplitude is reduced from 0.016 to about 0.011, with a central value of the observable velocity which decreases from 8.5 km/s to 7 km/s.

This irregular character of the observations has always represented a strong argument to interpret the small observed residuals as typical instrumental effects.
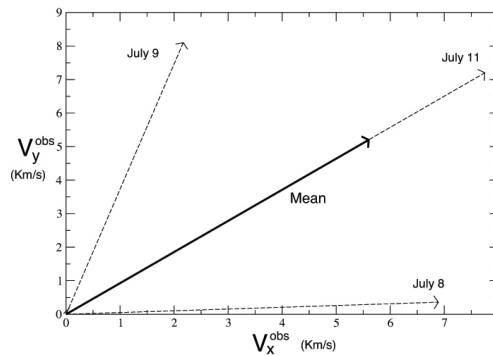

Fig. 8.   *The observable velocities for the three noon sessions of the Michelson-Morley experiment and their mean. The x-axis corresponds to $\theta_2 = 0^o \equiv 360^o$ and the y-axis to $\theta_2 = 270^o$. Statistical uncertainties of the various determinations are not reported. All individual directions could also be reversed by 180°. The figure is taken from.[7]*

3.2. *Further insights: Miller vs. Piccard-Stahel*

To get further insights we have compared two other sets of measurements, namely Miller's observations[35] and those performed by Piccard and Stahel.[39] Miller's large interferometer had an optical path of about 32 metres and was installed on top of Mount Wilson. His most extensive observations were made in blocks of ten days around April 1, August 1, September 15, 1925, and later on around February 8, 1926, with a total number of 6402 turns of the interferometer.[35] The result of his 1925 measurements, presented at the APS meeting in Kansas City on December 1925, was confirming his original claim of 1921, namely "there is a positive, systematic ether-drift effect, corresponding to a relative motion of the Earth and the ether, which at Mt. Wilson has an apparent velocity of 10 km/s".

Being aware that Miller's previous 1921 announcement of a non-zero ether-drift of about 9 km/s, if taken seriously, could undermine the basis of Einstein's relativity (Miller's results "carried a mortal blow to the theory of relativity"), Piccard and Stahel realized a precise apparatus with a small optical path of 280 cm that could be carried on board of a free atmospheric balloon (at heights of 2500 and 4500 m) to check the dependence on altitude. In this first series of measurements thermal disturbances were so strong that they could only set an upper limit of about 9 km/s to the magnitude of any ether-drift. However, after this first series of trials, precise observations were performed on dry land in Brussels and on top of Mt.Rigi in Switzerland (at an height of 1800 m).

Despite the optical path was much shorter than the size of the instruments used at that times in the United States, Piccard and Stahel were convinced that the precision of their measurements was higher because spurious disturbances were less important. In particular, with respect to the traditional direct observation, the fringe shifts were registered by photographic recording. Also, for thermal insulation, the interferometer was surrounded either by a thermostat filled with ice or by an iron enclosure where it could be possible to create a vacuum. This last solution was considered after having understood that the main instability in the fringe system was due to thermal disturbances in the air of the optical arms (rather than to temperature differences in the solid parts of the apparatus). However, very often the interference fringes were put out of order after few minutes by the presence of residual bubbles of air in the vacuum chamber. For this reason, they finally decided to run the experiment at atmospheric pressure with the ice thermostat which, by its great heat capacity, was found to stabilize the temperature in a satisfactory way.

We have thus considered the compatibility of these two experiments. Miller was always reporting his observations by quoting separately the amplitude and the phase of the individual sessions. In this way, as shown in Fig.4, the average observable velocity, obtained from a classical interpretation of his data, was $v_{\rm obs} \sim 8.4 \pm 2.2$ km/s. Piccard and Stahel were instead first performing a vector average of the data and, since the phase was found to vary in a completely arbitrary way, were quoting the much smaller value $v_{\rm obs} \sim (1.5 \div 1.7)$ km/s. For this reason, their measurements are traditionally considered a definite refutation of Miller.

But suppose that the ether-drift phenomenon has an intrinsic non-deterministic nature, which induces random fluctuations in the direction of the local drift. In this case, a vector average of the data from various sessions would completely obscure the physical information contained in the individual observations. For this reason, a meaningful comparison with Miller requires to apply his same procedure to the Piccard-Stahel data. Namely, first summarizing each measurement into a definite pair $(A_2^{\rm EXP}, \theta_2^{\rm EXP})$ for amplitude and azimuth, and then computing the magnitude of the observable velocity from the measured amplitudes. With this different procedure, the Piccard and Stahel observable velocity, at the 75% CL, becomes now
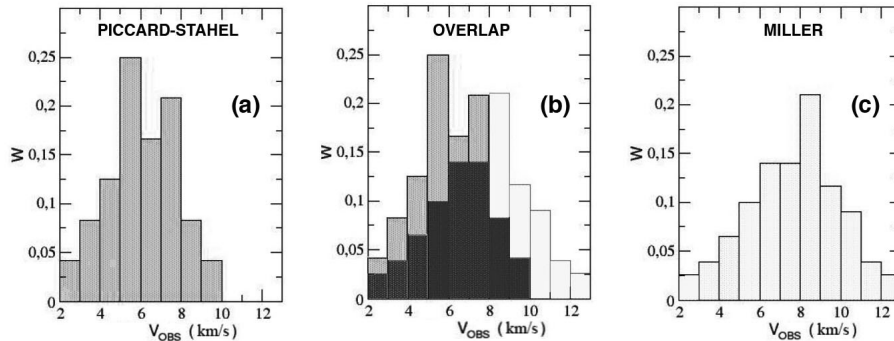
Fig. 9.   *We report in panel (a) the probability histogram W for the observable velocity obtained from the 24 individual amplitudes reported by Piccard and Stahel in.[39] In panel (c) we report the analogous histogram obtained from Miller's Figure 22d in.[35] In both cases, the vertical normalization is to a unit area. Finally, in panel (b) we report the overlap of the two histograms. The area of the overlap is 0.645. This gives a consistency between the two experiments of about 64%. The figure is taken from.[9]*

much larger, namely

$$v_{\mathrm{obs}} = 6.3^{+1.5}_{-2.0} \text{ km/s} \qquad\qquad (\mathrm{Piccard - Stahel}) \qquad (28)$$

and is now compatible with Miller's results. For a more refined test, we constructed probability histograms by considering the large set of measurements reported by Miller in Figure 22d of[35] and the 24 individual amplitudes reported by Piccard and Stahel in,[39] see Fig.9. From the area of the overlap, the consistency of the two experiments can be estimated to be about 64% which is a quite high level. At the same time, since the agreement is restricted to the region $v_{\mathrm{obs}} < 9$ km/s, Miller's higher values are likely affected by systematic disturbances. This would confirm Piccard and Stahel's claim that their apparatus, although of a smaller size, was more precise.

Therefore, summarizing, there is a range of observable velocity, say $v_{\mathrm{obs}} \sim 6.0 \pm 2.0$ km/s, where the results of the three experiments we have considered, namely Michelson-Morley, Miller and Piccard and Stahel, overlap consistently. This common range is obtained from the 2nd-harmonic amplitudes measured in a plenty of experimental sessions performed at different sidereal times and in different laboratories. As such, to a large extent, it should also be independent of spurious systematic effects. On the basis of Eq.(23), this range corresponds to a true kinematic velocity $v \sim 250 \pm 80$ km/s which could reasonably fit with the projection of the Earth velocity within the CMB at the various laboratories. Truly enough, this is only a first, partial view which must be supplemented by a deeper understanding of the observed random variability of the phase.
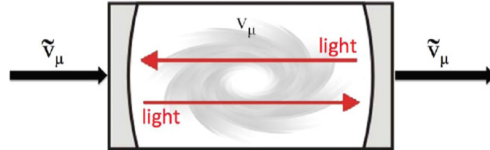
Fig. 10.   *The propagation of light in an optical cavity. It is emphasized that, independently of its particular name (physical vacuum, ether...) and differently from the solid parts of the apparatus, the underlying substrate is not completely entrained with the Earth motion. Thus, in general, its state of motion $v_\mu(t)$ is different from $\tilde{v}_\mu(t)$.*

4. Going deeper into the ether-drift phenomenon

The traditional expectation that an ether drift should precisely follow the smooth modulations induced by the Earth rotation, derives from the identification of the *local* velocity field which describes the drift in the plane of the interferometer, say $v_\mu(t)$, with the corresponding projection of the *global* Earth motion, say $\tilde{v}_\mu(t)$. By comparing with the motion of a macroscopic body in a fluid, this identification is equivalent to assume a form of regular, laminar flow, where global and local velocity fields coincide. Depending on the nature of the fluid, this assumption may be incorrect.

   To formulate an alternative model of ether drift, in refs.,[7–10] we started from Maxwell's original view[48] of light as a *wave process* which takes place in some substrate: "We are therefore obliged to suppose that the medium through which light is propagated is something distinct from the transparent media known to us". He was calling the underlying substrate 'ether' while, today, we prefer to call it 'physical vacuum'. However, this is irrelevant. The essential point for the propagation of light, e.g. inside an optical cavity, is that, differently from the solid parts of the apparatus, this physical vacuum is *not* completely entrained with the Earth motion see Fig.10.

   Thus, to explain the irregular character of the data, one could try to model the state of motion of the vacuum substrate as in a turbulent fluid[52, 53] or, more precisely, as in a fluid in the limit of zero viscosity. Then, the simple picture of a laminar flow is no more obvious due to the subtlety of the infinite-Reynolds-number limit, see e.g. Sect. 41.5 in Vol.II of Feynman's lectures.[54] In fact, beside the laminar regime where $v_\mu(t) = \tilde{v}_\mu(t)$, there is also another solution where $v_\mu(t)$ becomes a continuous but nowhere differentiable velocity field[55, 56] [m].

---

[m]The idea of the physical vacuum as an underlying stochastic medium, similar to a turbulent fluid, is deeply rooted in basic foundational aspects of both quantum physics and relativity. For
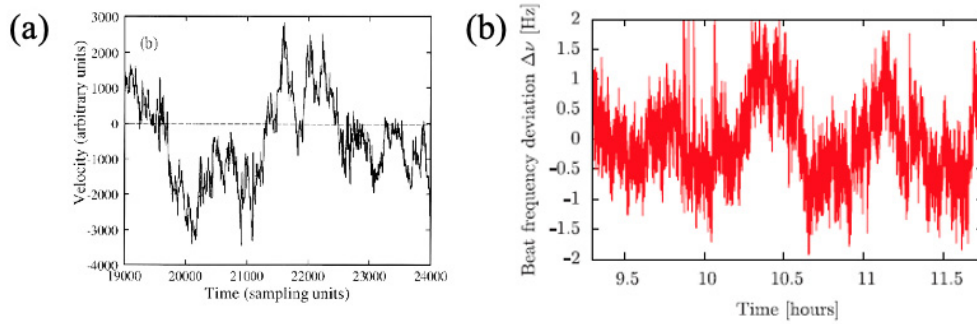
Fig. 11.   *We compare two different signals. Panel a) reports the turbulent velocity field measured in a wind tunnel.[67] Panel b) reports the instantaneous frequency shift measured with vacuum optical resonators in ref.[68] For the adopted laser frequency $\nu_0 = 2.8 \cdot 10^{14}$ Hz a $\Delta \nu = \pm 1$ Hz corresponds to a fractional value $\Delta \nu / \nu_0$ of about $\pm 3.5 \cdot 10^{-15}$.*

Together with these theoretical arguments, the analogy with a turbulent flow finds support in modern ether drift experiments where one measures the frequency shifts of two optical resonators. To this end, consider Fig.11. Panel a) reports the turbulent velocity field measured in a wind tunnel.[67] No doubt, this is a genuine signal, not noise. Panel b) reports instead the instantaneous frequency shift measured with vacuum optical cavities in ref.[68] So far, this other signal is interpreted as spurious noise.

Consider now Fig.12. Panel a) shows the power spectrum $S(\omega) \sim \omega^{-1.5}$ of the

instance, at the end of XIX century, the last model of the ether was a fluid full of very small whirlpools (a 'vortex-sponge').[57] The hydrodynamics of this medium was accounting for Maxwell equations and thus providing a model of Lorentz symmetry as emerging from a system whose elementary constituents are governed by Newtonian dynamics. In a different perspective, the idea of a quantum ether, as a medium subject to the fluctuations of the uncertainty relations, was considered by Dirac.[58] More recently, the model of turbulent ether has been re-formulated by Troshkin[59] (see also[60] and[61]) within the Navier-Stokes equation, by Saul[62] within Boltzmann's transport equation and in[63] within Landau's hydrodynamics. The same picture of the vacuum (or ether) as a turbulent fluid was Nelson's[64] starting point. In particular, the zero-viscosity limit gave him the motivation to expect that "the Brownian motion in the ether will not be smooth" and, therefore, to conceive the particular form of kinematics at the base of his stochastic derivation of the Schrödinger equation. A qualitatively similar picture is also obtained by representing relativistic particle propagation from the superposition, at short time scales, of non-relativistic particle paths with different Newtonian mass.[65] In this formulation, particles randomly propagate (as in a Brownian motion) in an underlying granular medium which replaces the trivial empty vacuum.[66]
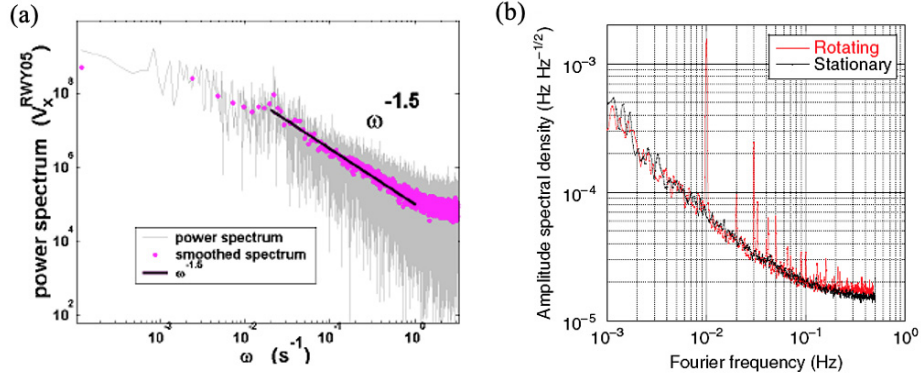
Fig. 12.   *We compare two different signals. Panel a) reports the power spectrum $S(\omega) \sim \omega^{-1.5}$ of the wind turbulence measured at the Florence Airport.[69] Panel b) shows the spectral amplitude $\sqrt{S(\omega)} \sim \omega^{-0.7}$ of the frequency shift measured by Nagel et al.[70] Above some minimal frequency the two curves reach a flat plateau. This corresponds to the maximum integration time beyond which the signal ceases to behave as a pure white-noise.*

wind turbulence measured at the Florence Airport.[69] No doubt, this is a physical signal. Panel b) shows the spectral amplitude $\sqrt{S(\omega)} \sim \omega^{-0.7}$ of the frequency shift measured by Nagel et al.[70] Again, this latter signal is interpreted as spurious noise.

Clearly these are just analogies but, very often, physical understanding proceeds by analogies. We have thus exploited the idea that the irregular signal observed in ether-drift experiments has a fundamental stochastic nature as when turbulence, at small scales, becomes statistically homogeneous and isotropic. With such an irregular signal numerical simulations are needed for a consistent description of the data. Therefore, for a check, one should first extract from the data the (2nd-harmonic) phase and amplitude and concentrate on the latter which is positive definite and remains non-zero under any averaging procedure. When measured at different times, this amplitude will anyhow exhibit modulations that, though indirectly, can provide information on the underlying cosmic motion.

To put things on a quantitative basis, let us assume the set of kinematic parameters $(V, \alpha, \gamma)_{\mathrm{CMB}}$ for the Earth motion in the CMB, a latitude ϕ of the laboratory and a given sidereal time $\tau = \omega_{\mathrm{sid}} t$ of the observations (with $\omega_{\mathrm{sid}} \sim \frac{2\pi}{23^h 56'}$). Then, for short-time observations of a few days, where the only time dependence is due to the Earth rotation, a simple application of spherical trigonometry[71] gives the projections in the (x, y) plane of the interferometer

$$\tilde{v}_x(t) = \tilde{v}(t) \cos \tilde{\theta}_2(t) = V \left[\sin \gamma \cos \phi - \cos \gamma \sin \phi \cos(\tau - \alpha) \right] \qquad (29)$$

$$\tilde{v}_y(t) = \tilde{v}(t) \sin \tilde{\theta}_2(t) = V \cos \gamma \sin(\tau - \alpha) \qquad (30)$$

with a magnitude

$$\tilde{v}(t) = V |\sin z(t)| \tag{31}$$

and

$$\cos z(t) = \sin \gamma \sin \phi + \cos \gamma \cos \phi \cos(\tau - \alpha) \tag{32}$$

As for the signal, let us also re-write Eq.(19) as

$$\frac{\Delta \bar{c}_\theta(t)}{c} \sim \epsilon \frac{v^2(t)}{c^2} \cos 2(\theta - \theta_2(t)) \tag{33}$$

where $v(t)$ and $\theta_2(t)$ now indicate respectively the magnitude and direction of the *local* drift in the same (x, y) plane of the interferometer. This can also be re-written as

$$\frac{\Delta \bar{c}_\theta(t)}{c} \sim 2S(t) \sin 2\theta + 2C(t) \cos 2\theta \tag{34}$$

with

$$2C(t) = \epsilon \, \frac{v_x^2(t) - v_y^2(t)}{c^2} \qquad 2S(t) = \epsilon \, \frac{2v_x(t)v_y(t)}{c^2} \tag{35}$$

and $v_x(t) = v(t) \cos \theta_2(t)$, $v_y(t) = v(t) \sin \theta_2(t)$.

In an analogy with a turbulent flow, the requirement of statistical isotropy means that the local quantities $v_x(t)$ and $v_y(t)$, which determine the observable properties of the drift, are very irregular functions that differ non trivially from their smooth, global counterparts $\tilde{v}_x(t)$ and $\tilde{v}_y(t)$, and can only be simulated numerically. To this end, a representation in terms of random Fourier series[55, 72, 73] was adopted in refs.[7–10] in a simplest uniform-probability model, where the kinematic parameters of the global $\tilde{v}_\mu(t)$ are just used to fix the boundaries for the local random $v_\mu(t)$. The basic ingredients are summarized in the Appendix.

In this model, the functions $S(t)$ and $C(t)$ have the characteristic behaviour of a *white-noise* signal with vanishing statistical averages $\langle C(t) \rangle_{\text{stat}} = 0$ and $\langle S(t) \rangle_{\text{stat}} = 0$ at *any* time t and whatever the global cosmic motion of the Earth. One can then understand the observed irregular behaviour of the fringe shifts

$$\frac{\Delta \lambda(\theta; t)}{\lambda} = \frac{2D}{\lambda} \left[2S(t) \sin 2\theta + 2C(t) \cos 2\theta \right] \tag{36}$$

In fact, their averages would be non vanishing just because the statistics is finite. Otherwise with more and more observations one would find

$$\langle \frac{\Delta \lambda(\theta; t)}{\lambda} \rangle_{\text{stat}} = \frac{2D}{\lambda} \left[2 \sin 2\theta \, \langle S(t) \rangle_{\text{stat}} + 2 \cos 2\theta \, \langle C(t) \rangle_{\text{stat}} \right] \to 0 \tag{37}$$

In particular, the direction $\theta_2(t)$ of the local drift, defined by the relation $\tan 2\theta_2(t) = S(t)/C(t)$, would vary randomly with no definite limit.

We have then checked the model by comparing with the amplitudes. Here we have first to consider the theoretical amplitude $\tilde{A}_2(t)$ associated with the global motion

$$\tilde{A}_2(t) \sim \frac{D}{\lambda} \cdot 2\epsilon \cdot \frac{V^2 \sin^2 z(t)}{c^2} \tag{38}$$

and then the amplitude $A_2(t)$ associated with the local non differentiable velocity components $v_x(t)$ and $v_y(t)$, Eqs.(83) and (84) of the Appendix

$$A_2(t) \sim \frac{D}{\lambda} \cdot 2\epsilon \cdot \frac{v_x^2(t) + v_y^2(t)}{c^2} \tag{39}$$

Clearly, the latter will exhibit sizeable fluctuations and be very different from the smooth $\tilde{A}_2(t)$. However, as shown in the Appendix, the relation between $\tilde{A}_2(t)$ and the statistical average $\langle A_2(t) \rangle_{\text{stat}}$ is extremely simple

$$\langle A_2(t) \rangle_{\text{stat}} = \frac{D}{\lambda} \cdot 2\epsilon \cdot \frac{\langle v_x^2(t) + v_y^2(t) \rangle_{\text{stat}}}{c^2} \sim \frac{\pi^2}{18} \cdot \tilde{A}_2(t) \tag{40}$$

so that, by averaging the amplitude at different sidereal times, one can obtain the crucial information on the angular parameters α and γ.

Altogether, the amplitudes of those old measurements can thus be interpreted in terms of three different velocities: a) as 6 ± 2 km/s in a classical picture b) as 250 ± 80 km/s, in a modern scheme and in a smooth picture of the drift c) as 340 ± 110 km/s, in a modern scheme but now allowing for irregular fluctuations of the signal. In fact, by replacing Eq.(38) with Eq.(40), from the same data, one would now obtain kinematical velocities which are larger by a factor $\sqrt{18/\pi^2} \sim 1.35$. In this third interpretation, the range of velocity agrees much better with the CMB value of 370 km/s.

To illustrate the agreement of our scheme with all classical measurements, we address to our book[9] where a detailed description is given of the experiments by Morley-Miller,[34] Miller,[35] Kennedy,[36] Illingworth,[37] Tomaschek[38] and Piccard-Stahel.[39] Instead, here, we will only consider the two most precise experiments that, traditionally, have been considered as definitely ruling out Miller's claims for a non-zero ether drift. Namely the Michelson-Pease-Pearson (MPP) observations at Mt. Wilson and the experiment performed in 1930 by Joos in Jena.[43] In particular, the latter remains incomparable among the classical experiments. To have an idea, Sommerfeld, being aware that the residuals in the Michelson-Morley data were not entirely negligible, concluded that only "After its repetition at Jena by Joos, the negative result of Michelson's experiment can be considered as definitely established" (A. Sommerfeld, Optics). However, there is again a subtlety because, as we shall see, Joos' experiment was *not* performed in the same conditions as the other experiments we have previously considered.

4.1. *Reanalysis of the MPP experiment*

To re-analyze the Michelson-Pease-Pearson (MPP) experiment, we first observe that no numerical results are reported in the original articles.[40,41] Instead, for more precise indications, one should look at Pease's paper.[42] There, one learns that they concentrated on a purely differential type of measurements. Namely, they were first statistically averaging the fringe shifts at those sidereal times that, according to
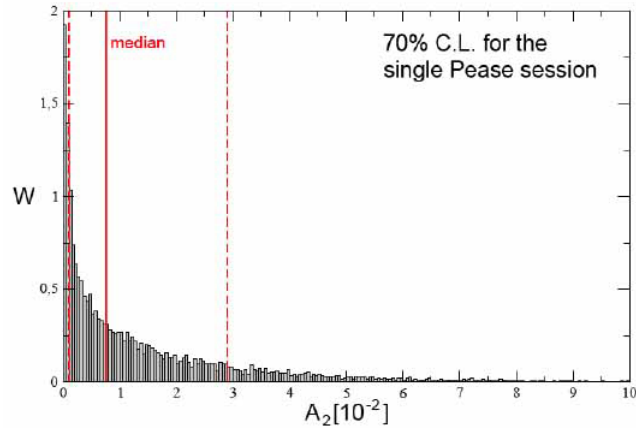
Fig. 13.   *The histogram W of a numerical simulation of 10,000 instantaneous amplitudes for the single session of January 13, 1928, reported by Pease[42] . The vertical normalization is to a unit area. We show the median and the 70% CL. The limits on the random Fourier components Eqs.(83) and (84) of the Appendix were fixed by inserting the CMB kinematical parameters in Eq.(87).*

Miller, were corresponding to maxima and minima of the ether-drift effect. Then, they were forming the difference

$$\delta(\theta) = \langle \frac{\Delta\lambda(\theta; t_{\max})}{\lambda} \rangle_{\text{stat}} - \langle \frac{\Delta\lambda(\theta; t_{\min})}{\lambda} \rangle_{\text{stat}} \tag{41}$$

which are the only numbers reported by Pease. These δ−values have a maximal magnitude of ± 0.004 and this is also the order of magnitude of the experimental amplitude $A_2^{\text{EXP}} \sim 0.005$ that is usually reported[74] for the MPP experiment when comparing with the much larger expected classical amplitudes $A_2^{\text{class}} \sim 0.45$ or $A_2^{\text{class}} \sim 0.29$ for optical paths of eighty-five or fifty-five feet respectively. Now, our stochastic, isotropic model predicts exactly zero statistical averages for vector quantities such as the fringe shifts, see Eq(37). Therefore, it would be trivial to reproduce the small δ-values in Eq.(41) in a numerical simulation with sufficiently high statistics. We have thus decided to compare instead with the only basic experimental session reported by Pease[42] (for optical path of fifty-five feet) which indicates a 2nd-harmonic amplitude $A_2^{\text{EXP}} \sim 0.006$. By comparing with the classical prediction for 30 km/s, namely $A_2^{\text{class}} \sim 0.29$, this amplitude corresponds to an observable velocity $v_{\text{obs}} \sim 4.3$ km/s but to a much larger value on the basis of Eq.(39).

Since we are dealing with a single measurement, to obtain a better understanding of its probability content, we have performed a direct numerical simulation by generating 10,000 values of the amplitude at the same sidereal time 5:30 of the MPP Mt. Wilson observation. The CMB kinematical parameters were used to bound the

random Fourier components of the stochastic velocity field Eqs.(83) and (84) of the Appendix. The resulting histogram is reported in Fig.13. From this histogram one obtains a mean simulated amplitude $\langle A_2^{\text{simul}} \rangle \sim 0.014$. This corresponds to replace the value of the scalar velocity $\tilde{v}(t) \sim 370$ km/s Eq.(77), at the sidereal time of Pease's observation, in the relation for the statistical average of the amplitude

$$\langle A_2(t) \rangle_{\text{stat}} = \frac{2\epsilon D}{\lambda} \frac{\langle v_x^2(t) + v_y^2(t) \rangle_{\text{stat}}}{c^2} \sim (1.6 \cdot 10^4) \cdot \frac{\pi^2}{18} \cdot \frac{\tilde{v}^2(t)}{c^2} \sim 0.009 \cdot \frac{\tilde{v}^2(t)}{(300 \text{ km/s})^2}$$
(42)

In the above relation we have replaced $D/\lambda \sim 2.9 \cdot 10^7$ (for optical path of fifty-five feet) and $\epsilon \sim 2.8 \cdot 10^{-4}$.

Note that the median of the amplitude distribution is about 0.007. As a consequence, the value $A_2^{\text{EXP}} \sim 0.006$ lies well within the 70% Confidence Limit. Also, the probability content becomes large at very small amplitudes [n] and there is a long tail extending up to about $A_2 \sim 0.030$.

The wide interval of amplitudes corresponding to the 70% C. L. indicates that, in our stochastic model, one could account for single observations that differ by an order of magnitude, say from 0.003 to 0.030. Thus, beside the statistical vanishing of vector quantities, this is another crucial difference with a purely deterministic model of the ether-drift. In this traditional view, in fact, within the errors, the amplitude can vary at most by a factor $r = (\tilde{v}_{\max}/\tilde{v}_{\min})^2$ where $\tilde{v}_{\max}$ and $\tilde{v}_{\min}$ are respectively the maximum and minimum of the projection of the Earth velocity Eq.(31). Since, for the known types of cosmic motion, one finds $r \sim 2$, the observation of such large fluctuations in the data would induce to conclude, in a deterministic model, that there is some systematic effect which affects the measurements in an uncontrolled way. With an ether drift of such irregular nature, it then becomes understandable the MPP reluctance to quote the individual results and instead report those particularly small combinations in Eq.(41) obtained by averaging and further subtracting large samples of data. This general picture of a highly irregular phenomenon is also confirmed by our reanalysis of Joos' experiment in the following subsection.

4.2. *Joos' experiment*

We will only give a brief description of Joos' 1930 experiment[43] and address to our book[9] for more details. Its sensitivity was about 1/3000 of a fringe, the fringes were recorded photographically with an automatic procedure and the optical system was enclosed in a hermetic housing. As reported by Miller,[35,75] it has been traditionally

---

[n]Strictly speaking, for a more precise description of the data, one should fold the histogram with a smearing function which takes into account the finite resolution Δ of the apparatus. This smearing would force the curve to bend for $A_2 \to 0$ and tend to some limit which depends on Δ. Nevertheless, this refinement should not modify substantially the probability content around the median which is very close to $A_2 = 0.007$.
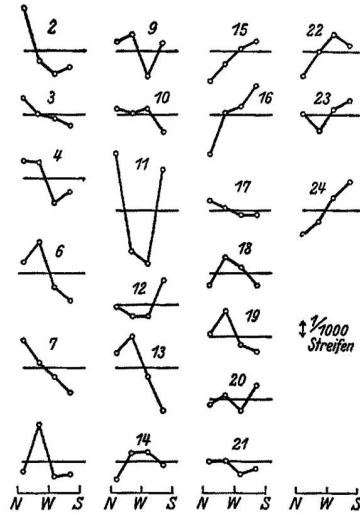
Fig. 14.   *The fringe shifts reported by Joos.[43] The yardstick corresponds to 1/1000 of a wavelength.*

believed that the measurements were performed in vacuum. In his article, however, Joos is not clear on this particular aspect. Only when describing his device for electromagnetic fine movements of the mirrors, he refers to the condition of an evacuated apparatus.[43] Instead, Swenson[76,77] declares that Joos' fringe shifts were finally recorded with optical paths placed in a helium bath. Therefore, we have decided to follow Swenson's explicit statements and assumed the presence of gaseous helium at atmospheric pressure.

From Eq.(40), by replacing $D/\lambda = 3.75 \cdot 10^7$ and the refractive index $\mathcal{N}_{\text{helium}} \sim 1.000033$ for gaseous helium, an average daily projection of the cosmic Earth velocity $\tilde{v}(t) = V|\sin z(t)| \sim 330$ km/s (appropriate for a Central-Europe laboratory) would provide the same amplitude as classically expected for the much smaller observable velocity of 2 km/s. We can thus understand the substantial reduction of the fringe shifts observed by Joos, with respect to the other experiments in air.

The data were taken at steps of one hour during the sidereal day and two observations (1 and 5) were finally deleted by Joos with the motivations that there were spurious disturbances, see Fig.14. From this picture, Joos adopted 1/1000 of a wavelength as upper limit and deduced the bound $v_{\text{obs}} \lesssim 1.5$ km/s. To this end, he was comparing with the classical expectation that, for his apparatus, a velocity of 30 km/s should have produced a 2nd-harmonic amplitude of 0.375 wavelengths. Though, since it is apparent that some fringe displacements were certainly larger than 1/1000 of a wavelength, we have performed 2nd-harmonic fits to Joos' data, see Fig.15. The resulting amplitudes are reported in Fig.16.

We note that a 2nd-harmonic fit to the large fringe shifts in picture 11 has a
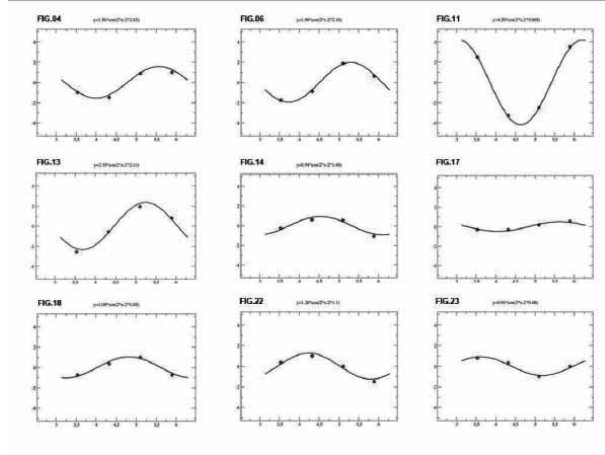
Fig. 15.   *Some 2nd-harmonic fits to Joos' data. The figure is taken from ref.*[9]
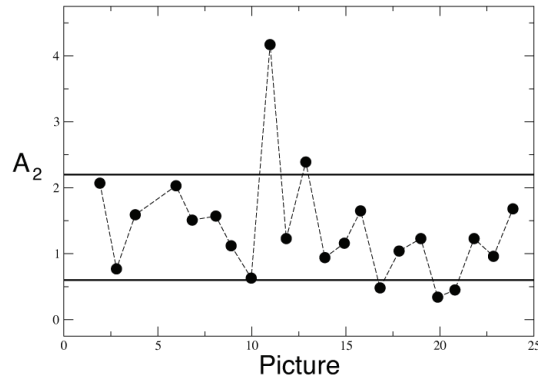

Fig. 16.   *Joos' 2nd-harmonic amplitudes, in units* 10^{-3}. *The vertical band between the two lines corresponds to the range* $(1.4 \pm 0.8) \cdot 10^{-3}$. *The uncertainty of each value is about* $\pm 3 \cdot 10^{-4}$. *The figure is taken from ref.*[7]

very good chi-square, comparable and often better than other observations with smaller values, see Fig.15. Therefore, there is no reason to delete the observation n.11. Its amplitude, however, $(4.1 \pm 0.3) \cdot 10^{-3}$ is abot ten times larger than the average amplitude $(0.4 \pm 0.3) \cdot 10^{-3}$ from the observations 20 and 21. This difference cannot be understood in a smooth model of the drift where, as anticipated, the projected velocity squared at the observation site can at most differ by a factor of two, as for the CMB motion at typical Central-Europe latitude where $(\tilde{v})_{\min} \sim 250$ km/s and $(\tilde{v})_{\max} \sim 370$ km/s. To understand these characteristic fluctuations, we have thus performed various numerical simulations of these amplitudes[7,9] in the

stochastic model described in the Appendix and using the kinematical parameters $(V, \alpha, \gamma)_{\mathrm{CMB}}$ to place the limits on the random velocity component Eqs.(83) and (84).

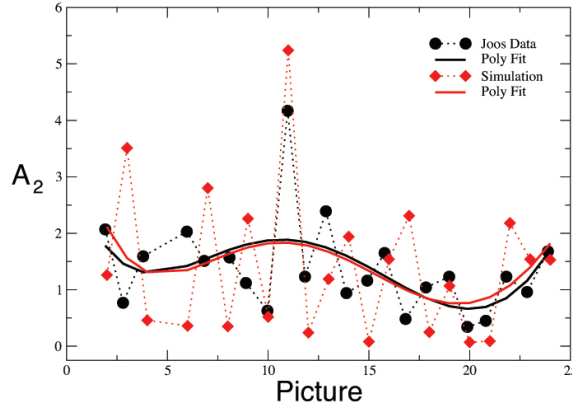Two simulations are shown in Figs.17 and 18 (the corresponding numerical values are reported in[7,9]).

Fig. 17.   *Joos' 2nd-harmonic amplitudes, in units 10^{-3} (black dots), are compared with a single simulation (red diamonds) at the same sidereal times of Joos' observations. Two 5th-order polynomial fits to the two sets of values are also shown. The figure is taken from ref.[7] .*

We want to emphasize two aspects. First, Joos' average amplitude $\langle A_2^{\mathrm{EXP}} \rangle = (1.4 \pm 0.8) \cdot 10^{-3}$ when compared with the classical prediction for his interferometer $A_2^{\mathrm{class}} = \frac{D}{\lambda} \frac{(30\mathrm{km/s})^2}{c^2} \sim 0.375$ gives indeed an observable velocity $v_{\mathrm{obs}} \sim (1.8 \pm 0.5)$ km/s very close to the 1.5 km/s value quoted by Joos. But, when comparing with our prediction in the stochastic model Eq.(40) one would now find a true kinematical velocity $\tilde{v} = 305^{+85}_{-100}$ km/s. Second, when fitting with Eqs.(76) and (77) the smooth black curve of the Joos data in Fig.17 one finds[7] a right ascension $\alpha(\mathrm{fit} - \mathrm{Joos}) = (168 \pm 30)$ degrees and an angular declination $\gamma(\mathrm{fit} - \mathrm{Joos}) = (-13 \pm 14)$ degrees which are consistent with the present values $\alpha(\mathrm{CMB}) \sim 168$ degrees and $\gamma(\mathrm{CMB}) \sim -7$ degrees. This confirms that, when studied at different sidereal times, the measured amplitude can provide precious information on the angular parameters.

4.3. *Summary of all classical experiments*

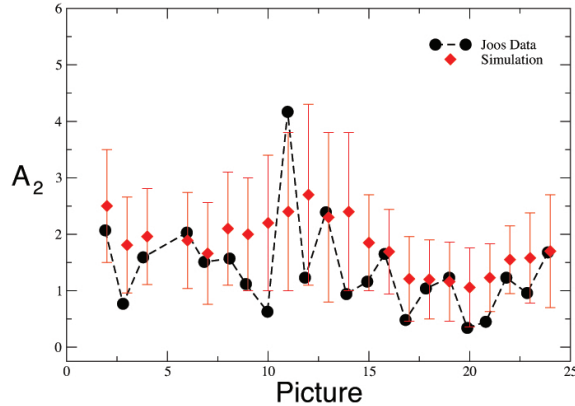A comparison with all classical experiments is finally shown in Table 3.

Fig. 18.   *Joos' 2nd-harmonic amplitudes in units 10^{-3} (black dots) are now compared with a simulation where one averages ten measurements, performed on 10 consecutive days, at the same sidereal times of Joos' observations (red diamonds). The change of the averages observed by varying the parameters of the simulation was summarized into a central value and a symmetric error. The figure is taken from ref.[7]*

Note the substantial difference with the analogous summary Table I of ref.[74] where those authors were comparing with the classical amplitudes Eq.(22) and emphasizing the much smaller magnitude of the experimental fringes. Here, is just the opposite. In fact, our theoretical statistical averages are often *smaller* than the experimental results indicating, most likely, the presence of systematic effects in the measurements.

At the same time, by adopting Eq.(40), we find $\tilde{v}_{\exp} \sim 418 \pm 62$ km/s from all experiments in air and $\tilde{v}_{\exp} \sim 323 \pm 70$ km/s from the two experiments in gaseous helium, with a global average $\langle \tilde{v}_{\exp} \rangle \sim 376 \pm 46$ km/s which agrees well with the 370 km/s from the CMB observations. Even more, from the two most precise experiments of Piccard-Stahel (Brussels and Mt.Rigi) and Joos (Jena), we find two determinations, $\tilde{v}_{\exp} = 360^{+85}_{-110}$ km/s and $\tilde{v}_{\exp} = 305^{+85}_{-100}$ km/s respectively, whose average $\langle \tilde{v} \rangle \sim 332^{+60}_{-80}$ km/s reproduces to high accuracy the projection of the CMB velocity at a typical Central-Europe latitude.

4.4. *The intriguing role of temperature*

As anticipated in Sect.2 (see footnote [k]), symmetry arguments can successfully describe a phenomenon regardless of the physical mechanisms behind it. The same is true here with our relation $\frac{|\Delta \bar{c}_\theta|}{c} \sim \epsilon(v^2/c^2)$ in Eq.(19). It works but does *not* explain the ultimate origin of the small effects observed in the gaseous systems. For instance, as a first mechanism, we considered the possibility of different polarizations in different directions in the dielectric, depending on its state of motion. But, if this works in weakly bound gaseous matter, the same mechanism should also work in

Table 3.   The average 2nd-harmonic amplitudes of classical ether-drift experiments. These were extracted from the original papers by averaging the amplitudes of the individual observations and assuming the direction of the local drift to be completely random (i.e. no vector averaging of different sessions). These experimental values are then compared with the full statistical average Eq.(40) for a projection 250 km/s $\lesssim \tilde{v} \lesssim$ 370 km/s of the Earth motion in the CMB and refractivities $\epsilon = 2.8 \cdot 10^{-4}$ for air and $\epsilon = 3.3 \cdot 10^{-5}$ for gaseous helium. The experimental value for the Morley-Miller experiment is taken from the observed velocities reported in Miller's Figure 4, here our Fig.4. The experimental value for the Michelson-Pease–Pearson experiment refers to the only known session for which the fringe shifts are reported explicitly[42] and where the optical path was still fifty-five feet. The symbol $\pm....$ means that the experimental uncertainty cannot be determined from the available informations. The table is taken from ref.[10]

Experiment	gas	A_2^{EXP}	$\frac{2D}{\lambda}$	$\langle A_2(t)\rangle_{\text{stat}}$
Michelson(1881)	air	$(7.8 \pm ....) \cdot 10^{-3}$	$4 \cdot 10^6$	$(0.7 \pm 0.2) \cdot 10^{-3}$
Michelson-Morley(1887)	air	$(1.6 \pm 0.6) \cdot 10^{-2}$	$4 \cdot 10^7$	$(0.7 \pm 0.2) \cdot 10^{-2}$
Morley-Miller(1902-1905)	air	$(4.0 \pm 2.0) \cdot 10^{-2}$	$1.12 \cdot 10^8$	$(2.0 \pm 0.7) \cdot 10^{-2}$
Miller(1921-1926)	air	$(4.4 \pm 2.2) \cdot 10^{-2}$	$1.12 \cdot 10^8$	$(2.0 \pm 0.7) \cdot 10^{-2}$
Tomaschek (1924)	air	$(1.0 \pm 0.6) \cdot 10^{-2}$	$3 \cdot 10^7$	$(0.5 \pm 0.2) \cdot 10^{-2}$
Kennedy(1926)	helium	< 0.002	$7 \cdot 10^6$	$(1.4 \pm 0.5) \cdot 10^{-4}$
Illingworth(1927)	helium	$(2.2 \pm 1.7) \cdot 10^{-4}$	$7 \cdot 10^6$	$(1.4 \pm 0.5) \cdot 10^{-4}$
Piccard-Stahel(1928)	air	$(2.8 \pm 1.5) \cdot 10^{-3}$	$1.28 \cdot 10^7$	$(2.2 \pm 0.8) \cdot 10^{-3}$
Mich.-Pease-Pearson(1929)	air	$(0.6 \pm ...) \cdot 10^{-2}$	$5.8 \cdot 10^7$	$(1.0 \pm 0.4) \cdot 10^{-2}$
Joos(1930)	helium	$(1.4 \pm 0.8) \cdot 10^{-3}$	$7.5 \cdot 10^7$	$(1.5 \pm 0.6) \cdot 10^{-3}$

a strongly bound solid dielectric, where the refractivity is $(\mathcal{N}_{\text{solid}} - 1) = O(1)$, and thus produce a much larger $\frac{|\Delta \bar{c}_\theta|}{c} \sim (\mathcal{N}_{\text{solid}} - 1)(v^2/c^2) \sim 10^{-6}$. This is in contrast with the Shamir-Fox[78] experiment in perspex where the observed value was smaller by orders of magnitude.

We have thus re-considered[8,9,79] the traditional thermal interpretation[74,80] of the observed residuals. The idea was that, in a weakly bound system as a gas, a small temperature difference $\Delta T^{\text{gas}}(\theta)$ in the air of the two optical arms produces a difference in the refractive index and a $(\Delta \bar{c}_\theta/c) \sim \epsilon_{\text{gas}} \Delta T^{\text{gas}}(\theta)/T$, where $T \sim$ 300 K is the absolute temperature of the laboratory º. Miller was aware[35,75] that his results could be due to a $\Delta T^{\text{gas}}(\theta) \lesssim 1$ mK but objected that casual changes of the ambiance temperature would largely cancel when averaging over many measurements. Only temperature effects with a definite periodicity would survive. For a quantitative estimate, by averaging over all experiments in Table 3 we found $\langle \tilde{v}_{\text{exp}} \rangle \sim 376 \pm 46$ km/s. Therefore, by comparing Eq.(40) with the corresponding

---

ºThe starting point is the Lorentz-Lorenz equation for the molecular polarizability in the ideal-gas approximation (as for air or gaseous helium at atmospheric pressure), see[8,9] for the details.

form for a thermal light anisotropy, we find

$$\frac{|\Delta \bar{c}_\theta|}{c} \sim \epsilon_{\text{gas}} \frac{\pi^2}{18} \frac{\langle \tilde{v}_{\text{exp}} \rangle^2}{c^2} \sim \epsilon_{\text{gas}} \frac{|\Delta T^{\text{gas}}(\theta)|}{T} \tag{43}$$

and a value[8,9] $|\Delta T^{\text{gas}}(\theta)| \sim (0.26 \pm 0.07)$ mK [p].

This motivates the following two observations. First, after a century from those old measurements, in a typical room-temperature laboratory environment, a stability at the level of a fraction of millikelvin is still state of the art, see.[81–83] This would support the idea that we are dealing with a non-local effect that places a fundamental limit.

Second, as for possible dynamical explanations, we mentioned in footnote [k] a collective interaction of the gaseous system with hypothetical dark matter in the Galaxy or with the CMB radiation. For the consistency with the velocity of 370 km/s, the latter hypothesis seems now more plausible. In this interpretation, these interactions would be so weak that, on average, the induced temperature differences in the optical paths are only 1/10 of the whole $\Delta T^{\text{CMB}}(\theta)$ in Eq.(3).

Nevertheless, whatever its precise origin, this thermal explanation can help intuition. In fact, it can explain the *quantitative* reduction of the effect in the vacuum limit where $\epsilon_{\text{gas}} \to 0$ and the *qualitative* difference with solid dielectric media where temperature differences of a fraction of millikelvin cannot produce any appreciable deviation from isotropy in the rest frame of the medium.

Admittedly, the idea that small modifications of gaseous matter, produced by the tiny CMB temperature variations, can be detected by precise optical measurements in a laboratory, while certainly unconventional, has not the same implications of a genuine preferred-frame effect due to the vacuum structure. Still, this thermal explanation of the small residuals in gases, very recently reconsidered by Manley,[84] has a crucial importance. In fact, it implies that if a tiny, but non-zero, fundamental signal could definitely be detected in vacuum then, with very precise measurements, the *same* universal signal should also show up in a *solid dielectric* where a disturbing ΔT of a fraction of millikelvin becomes irrelevant. Detecting such 'non-thermal' light anisotropy, for the same cosmic motion indicated by the CMB observations, is thus necessary to confirm the idea of a fundamental preferred frame.

5. The modern ether-drift experiments

Searching for a 'non-thermal' light anisotropy, which could be detected with light propagating in vacuum and/or in solid dielectrics, we will now compare with the modern experiments[44] where $\frac{\Delta \bar{c}_\theta}{c} \sim \frac{\Delta \nu(\theta)}{\nu_0}$ is now extracted from the frequency shift of two optical resonators, see Fig.3. The particular type of laser-cavity coupling used in the experiments is known in the literature as the Pound-Drever-Hall system,[85,86]

---

[p]Note that in Eq.(43) the gas refractivity drops out. The old estimates[74,80] of about 1 mK, based on the relation $\epsilon_{\text{gas}} \Delta T^{\text{gas}}(\theta)/T \sim (v_{\text{Miller}}^2/2c^2)$, with $v_{\text{Miller}} \sim 10$ km/s, were slightly too large.

see Black's tutorial article[87] for a beautiful introduction. A laser beam is sent into a Fabry-Perot cavity which acts as a filter. Then, a part of the output of the cavity is fed back to the laser to suppress its frequency fluctuations. This method provides a very narrow bandwidth and has been crucial for the precision measurements we are going to describe.

The first application to the ether-drift experiments was realized by Brillet and Hall in 1979.[88] They were comparing the frequency of a CH_4 reference laser (fixed in the laboratory) with the frequency of a cavity-stabilized He-Ne laser ($\nu_0 \sim 8.8 \cdot 10^{13}$ Hz) placed on a rotating table. Since the stabilizing optical cavity was placed inside a vacuum envelope, the measured shift $\Delta\nu(\theta)$ was giving a measure of the anisotropy of the velocity of light in vacuum. The short-term stability of the cavity-laser system was found to be about $\pm$ 20 Hz for a 1-second measurement, and comparable to the stability of the reference CH_4 laser. It was also necessary to correct the data for a substantial linear drift of about 50 Hz/s.

By grouping the data in blocks of 10-20 rotations they found a signal with a typical amplitude $|\Delta\nu| \sim 17$ Hz (or a relative level 10^{-13}) and with a phase $\theta_2(t)$ which was randomly varying. Therefore, by increasing the statistics and projecting along the axis corresponding to the Earth cosmic velocity obtained from the first CMB observations,[89] the surviving average effect was substantially reduced down to about ± 1 Hz. Finally, by further averaging over a period of about 200 days, the residual ether-drift effect was an average frequency shift $\langle\Delta\nu\rangle = 0.13 \pm 0.22$ Hz, i.e. about 100 times smaller than the instantaneous $|\Delta\nu|$.

Since the 1979 Brillet-Hall article, substantial improvements have been introduced in the experiments. Just to have an idea, in present-day measurements[68,90] with vacuum cavities the typical magnitude of the instantaneous fractional signal $|\Delta\nu|/\nu_0$ has been lowered from 10^{-13} to 10^{-15}, the linear drift from 50 Hz/s to about 0.05 Hz/s and, after averaging over many observations, the best limit which is reported is a residual $\langle\frac{\Delta\nu}{\nu_0}\rangle \lesssim 10^{-18}$,[68] i.e. about 1000 times smaller than the instantaneous 10^{-15} signal.

The assumptions behind the analysis of the data, however, are basically unchanged. In fact, a genuine ether drift is always assumed to be a regular phenomenon depending deterministically on the Earth cosmic motion and averaging more and more observations is considered a way of improving the accuracy. But, as emphasized in Sect.4, the classical experiments indicate genuine physical fluctuations that are *not* spurious noise but, instead, express how the cosmic motion of the Earth is actually seen in a detector. For this reason, we will first consider the instantaneous signal and try to understand if it can admit a physical interpretation.

5.1. *A 10^{-9} refractivity for the vacuum (on the Earth surface)*

As anticipated, after averaging many observations, the best limit which is reported for measurements with vacuum resonators is a residual $\langle\Delta\nu/\nu_0\rangle \lesssim 10^{-18}$.[68] This just reflects the very irregular nature of the signal because its typical magnitude

$|\Delta\nu|/\nu_0 \sim 10^{-15}$ is about 1000 times larger, see Fig.19 or panel b) of Fig.11.
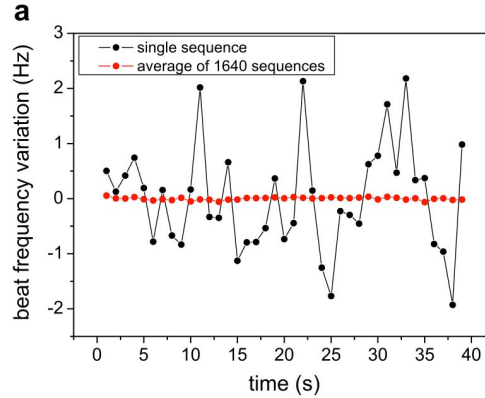

Fig. 19.   *The experimental frequency shift reported in Fig.9(a) of ref.[90] (courtesy Optics Communications). The black dots give the instantaneous signal, the red dots give the signal averaged over 1640 sequences. For a laser frequency $\nu_0 = 2.8 \cdot 10^{14}$ Hz a $\Delta\nu = \pm 1$ Hz corresponds to a fractional value $\Delta\nu/\nu_0$ of about $\pm 3.5 \cdot 10^{-15}$.*

The most interesting aspect however is that this 10^{-15} instantaneous signal, found in the room-temperature experiments of refs.[90] and,[68] was also found in ref.[91] where the solid parts of the vacuum resonators were made of different material and even in ref.[92] were the apparatus was operating in the *cryogenic* regime. Since it is very unlike that spurious effects (e.g. thermal noise[93]) remain the same for experiments operating in so different conditions, one can meaningfully explore the possibility that such an irregular 10^{-15} signal admits a physical interpretation.

In the same model discussed for the classical experiments, we are then lead to the concept of a refractive index $\mathcal{N}_v = 1 + \epsilon_v$ for the vacuum or, more precisely, for the physical vacuum established in an optical cavity, as in Fig.10, when this is placed on the Earth surface. The refractivity ϵ_v should be at the 10^{-9} level, in order to give $\frac{|\Delta\bar{c}_\theta|}{c} \sim \epsilon_v \ (v^2/c^2) \ \sim 10^{-15}$ and thus would fit with the original idea of[94] where, for an apparatus placed on the Earth's surface, a vacuum refractivity $\epsilon_v \sim (2G_N M/c^2 R) \sim 1.39 \cdot 10^{-9}$ was considered, G_N being the Newton constant and M and R the mass and radius of the Earth. Since this idea will sound unconventional to many readers, we have first to recall the main motivations.

An effective refractivity for the physical vacuum becomes a natural idea when adopting a different view of the curvature effects observed in a gravitational field. In General Relativity these curvature effects are viewed as a fundamental modification of Minkowski space-time. However, it is an experimental fact that many physical systems for which, at a fundamental level, space-time is exactly flat are nevertheless described by an effective curved metric in their hydrodynamic limit, i.e. at length

scales much larger than the size of their elementary constituents. For this reason, several authors, see e.g.,[95–97] have explored the idea that Einstein gravity might represent an emergent phenomenon and started to considered those gravity-analogs (moving fluids, condensed matter systems with a refractive index, Bose-Einstein condensates,...) which are known in flat space.

The main ingredient of this approach consists in the introduction of some background fields $s_k(x)$ in flat space expressing the deviations of the effective metric $g_{\mu\nu}(x)$ from the Minkowski tensor $\eta_{\mu\nu}$, i.e.

$$g_{\mu\nu}(x) - \eta_{\mu\nu} = \delta g_{\mu\nu}[s_k(x)] \qquad (44)$$

with $\delta g_{\mu\nu}[s_k = 0] = 0$. In this type of approach, to (partially) fill the conceptual gap with classical General Relativity, as in the original Yilmaz derivation,[98] one could impose that Einstein's equations for the metric become *algebraic identities* which follow directly from the equations of motion for the s_k's in flat space, after introducing a suitable stress tensor $t^\mu_\nu(s_k)$ [q].

As an immediate consequence, suppose that the s_k's represent *excitations* of the physical vacuum which therefore vanish identically in the equilibrium state. Then, if curvature effects are only due to departures from the lowest-energy state, one could immediately understand[97] why the huge condensation energy of the unperturbed vacuum plays no role and thus obtain an intuitive solution of the cosmological-constant problem found in connection with the vacuum energy [r].

Here, in our context of the ether-drift experiments, we will limit ourselves to explore some phenomenological consequence of this picture. To this end, let us assume a zeroth-order model of gravity with a scalar field $s_0(x)$ which behaves as the Newtonian potential (at least on some coarse-grained scale and consistently with the experimental verifications of the 1/r law at the sub-millimeter level[100]). How could the effects of $s_0(x)$ be effectively re-absorbed into a curved metric structure? At a pure geometrical level and regardless of the detailed dynamical mechanisms, the standard basic ingredients would be: 1) space-time dependent modifications of the physical clocks and rods and 2) space-time dependent modifications of the velocity of light [s].

---

[q]In the simplest, original Yilmaz approach[98] there is only one inducing-gravity field $s_0(x)$ which plays the role of the Newtonian potential. Introducing its stress tensor $t^\mu_\nu(s_0) = -\partial^\mu s_0 \partial_\nu s_0 + 1/2\delta^\mu_\nu \, \partial^\alpha s_0 \partial_\alpha s_0$, to match the Einstein tensor, produces differences from the Schwarzschild metric which are beyond the present experimental accuracy.

[r]This is probably the simplest way to follow Feynman's indication: "The first thing we should understand is how to formulate gravity so that it doesn't interact with the vacuum energy".[99]

[s]This point of view can be well represented by some citations. For instance, "It is possible, on the one hand, to postulate that the velocity of light is a universal constant, to define *natural* clocks and measuring rods as the standards by which space and time are to be judged and then to discover from measurement that space-time is *really* non-Euclidean. Alternatively, one can *define* space as Euclidean and time as the same everywhere, and discover (from exactly the same

Within this interpretation, one could thus try to check the fundamental assumption of General Relativity that, even in the presence of gravity, the velocity of light in vacuum c_γ is a universal constant, namely it remains the same, basic parameter c entering Lorentz transformations. Notice that, here, we are not considering the so called coordinate-dependent speed of light. Rather, our interest is focused on the value of the true, physical c_γ as, for instance, obtained from experimental measurements in vacuum optical cavities placed on the Earth surface.

To spell out the various aspects, a good reference is Cook's article "Physical time and physical space in general relativity".[103] This article makes extremely clear which definitions of time and length, respectively dT and dL, are needed if all observers have to measure the same, universal speed of light ("Einstein postulate"). For a static metric, these definitions are $dT^2 = g_{00}dt^2$ and $dL^2 = g_{ij}dx^i dx^j$. Thus, in General Relativity, the condition $ds^2 = 0$, which governs the propagation of light, can be expressed formally as

$$ds^2 = c^2 dT^2 - dL^2 = 0 \tag{45}$$

and, by construction, yields the same universal speed $c = dL/dT$.

For the same reason, however, if the physical units of time and space were instead defined to be $d\hat{T}$ and $d\hat{L}$ with, say, $dT = q\ d\hat{T}$ and $dL = p\ d\hat{L}$, the same condition

$$ds^2 = c^2 q^2 d\hat{T}^2 - p^2 d\hat{L}^2 = 0 \tag{46}$$

would now be interpreted in terms of the different speed

$$c_\gamma = \frac{d\hat{L}}{d\hat{T}} = c\ \frac{q}{p} \equiv \frac{c}{\mathcal{N}_v} \tag{47}$$

The possibility of different standards for space-time measurements is thus a simple motivation for an effective vacuum refractive index $\mathcal{N}_v \neq 1$.

With these premises, the unambiguous point of view of Special Relativity is that the right space-time units are those for which the speed of light in the vacuum c_γ, when measured in an inertial frame, coincides with the basic parameter c entering Lorentz transformations. However, inertial frames are just an idealization. Therefore the appropriate realization is to assume *local* standards of distance and time such that the identification $c_\gamma = c$ holds as an asymptotic relation in the physical conditions which are as close as possible to an inertial frame, i.e. *in a freely falling frame* (at least by restricting light propagation to a space-time region small enough that

measurements) how the velocity of light and natural clocks, rods and particle inertias *really* behave in the neighborhood of large masses".[101] Or "Is space-time really curved? Isn't it conceivable that space-time is actually flat, but clocks and rulers with which we measure it, and which we regard as perfect, are actually rubbery? Might not even the most perfect of clocks slow down or speed up and the most perfect of rulers shrink or expand, as we move them from point to point and change their orientations? Would not such distortions of our clocks and rulers make a truly flat space-time appear to be curved? Yes."[102]
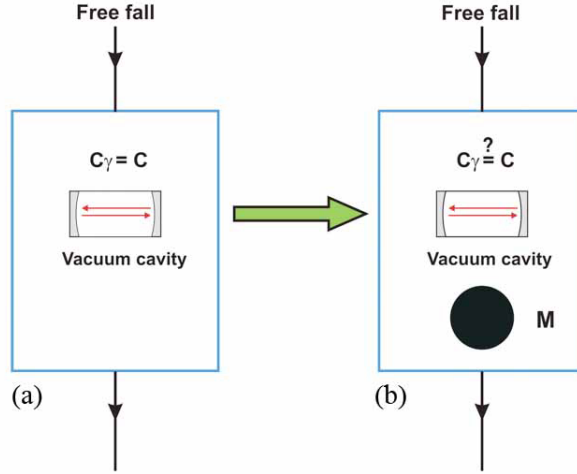
Fig. 20.   *A pictorial representation of the effect of a heavy mass M carried on board of a freely-falling system, case (b). With respect to the ideal case (a), the mass M modifies the local space-time units and could introduce a vacuum refractivity so that now $c_\gamma \neq c$.*

tidal effects of the external gravitational potential $U_{\text{ext}}(x)$ can be ignored). Note that this is essential to obtain an operational definition of the otherwise *unknown* parameter c.

As already discussed in ref.,[94] light propagation for an observer S sitting on the Earth's surface can then be described with increasing degrees of accuracy starting from step i), through ii) and finally arriving to iii):

i) S is considered a freely falling frame. This amounts to assume $c_\gamma = c$ so that, given two events which, in terms of the local space-time units of S, differ by (dx, dy, dz, dt), light propagation is described by the condition (ff='free-fall')

$$(ds^2)_{\text{ff}} = c^2 dt^2 - (dx^2 + dy^2 + dz^2) = 0 \tag{48}$$

ii) To a closer look, however, an observer S placed on the Earth surface can only be considered a freely-falling frame up to the presence of the Earth gravitational field. Its inclusion can be estimated by considering S as a freely-falling frame, in the same external gravitational field described by $U_{\text{ext}}(x)$, that however is also carrying on board a heavy object of mass M (the Earth mass itself) which affects the local space-time structure, see Fig.20. To derive the required correction, let us denote by δU the extra Newtonian potential produced by the heavy mass M at the experimental set up where one wants to describe light propagation. According to General Relativity, and to first order in δU, light propagation for the S observer is

now described by

$$ds^2 = c^2 dt^2 (1 - 2\frac{|\delta U|}{c^2}) - (dx^2 + dy^2 + dz^2)(1 + 2\frac{|\delta U|}{c^2}) \equiv c^2 dT^2 - dL^2 = 0 \quad (49)$$

where $dT^2 = (1 - 2\frac{|\delta U|}{c^2})dt^2$ and $dL^2 = (1 + 2\frac{|\delta U|}{c^2})(dx^2 + dy^2 + dz^2)$ are the physical units of General Relativity in terms of which one obtains the universal value $dL/dT = c_\gamma = c$.

Though, to check *experimentally* the assumed identity $c_\gamma = c$ one should compare with a theoretical prediction for $(c - c_\gamma)$ and thus *necessarily* modify some formal ingredient of General Relativity. As a definite possibility, let us maintain the same definition of the unit of length $d\hat{L} = dL$ but change the unit of time from dT to $d\hat{T}$. The reason derives from the observation that physical units of time scale as inverse frequencies and that the measured frequencies $\hat{\omega}$ for $\delta U \neq 0$, when compared to the corresponding value ω for $\delta U = 0$, are *red-shifted* according to

$$\hat{\omega} = (1 - \frac{|\delta U|}{c^2}) \, \omega \quad (50)$$

Therefore, rather than the *natural* unit of time $dT = (1 - \frac{|\delta U|}{c^2})dt$ of General Relativity, one could consider the alternative, but natural (see our footnote [s]), unit of time

$$d\hat{T} = (1 + \frac{|\delta U|}{c^2}) \, dt \quad (51)$$

Then, to reproduce $ds^2 = 0$, we can introduce a vacuum refractive index

$$\mathcal{N}_v \sim 1 + 2\frac{|\delta U|}{c^2} \quad (52)$$

so that the *same* Eq.(49) takes now the form

$$ds^2 = \frac{c^2 d\hat{T}^2}{\mathcal{N}_v^2} - d\hat{L}^2 = 0 \quad (53)$$

This gives $d\hat{L}/d\hat{T} = c_\gamma = \frac{c}{\mathcal{N}_v}$ and, for an observer placed on the Earth's surface, a refractivity

$$\epsilon_v = \mathcal{N}_v - 1 \sim \frac{2G_N M}{c^2 R} \sim 1.39 \cdot 10^{-9} \quad (54)$$

M and R being respectively the Earth mass and radius.

Notice that, with this natural definition $d\hat{T}$, the vacuum refractive index associated with a Newtonian potential is the same usually reported in the literature, at least since Eddington's 1920 book,[104] to explain in flat space the observed deflection of light in a gravitational field. The same expression is also suggested by the formal analogy of Maxwell equations in General Relativity with the electrodynamics of a macroscopic medium with dielectric function and magnetic permeability[105]

$\epsilon_{ik} = \mu_{ik} = \sqrt{-g} \ \frac{(-g^{ik})}{g_{00}}$. Indeed, in our case, from the relations $g^{il}g_{lk} = \delta^i_k$, $(-g^{ik}) \sim \delta^i_k \ g_{00}$, $\epsilon_{ik} = \mu_{ik} = \delta^i_k \mathcal{N}_v$, we obtain

$$\mathcal{N}_v \sim \sqrt{-g} \sim \sqrt{(1 - 2\frac{|\delta U|}{c^2})(1 + 2\frac{|\delta U|}{c^2})^3} \sim 1 + 2\frac{|\delta U|}{c^2} \tag{55}$$

A difference is found with Landau's and Lifshitz' textbook[107] where the vacuum refractive index entering the constitutive relations is instead defined as $\mathcal{N}_v \sim \frac{1}{\sqrt{g_{00}}} \sim 1 + \frac{|\delta U|}{c^2}$. Concerning, these two possible definitions of $\mathcal{N}_v$, we address the reader to Broekaert's article,[106] see his footnote 3, where a very complete set of references for the vacuum refractive index in gravitational field is reported. However, this difference of a factor of 2 is not really essential and can be taken into account as a theoretical uncertainty. The main point is that c_γ, as measured in a vacuum cavity on the Earth's surface (panel **(b)** in our Fig.20), could differ at a fractional level 10^{-9} from the ideal value c, as operationally defined with the same apparatus in a true freely-falling frame (panel **(a)** in our Fig.20). In conclusion, this $c_\gamma - c$ difference can be conveniently expressed through a vacuum refractivity of the form

$$\epsilon_v = \mathcal{N}_v - 1 \sim \frac{\chi}{2} \ 1.39 \cdot 10^{-9} \tag{56}$$

where the factor $\chi/2$ (with $\chi = 1$ or 2) takes into account the mentioned theoretical uncertainty.

iii) Could one check experimentally if $\mathcal{N}_v \neq 1$? Today, the speed of light in vacuum is assumed to be a fixed number with no error, namely 299 792 458 m/s. Thus if, for instance, this estimate were taken to represent the value measured on the Earth surface, in an ideal freely-falling frame there could be a slight increase, namely $+\frac{\chi}{2}(0.42)$ m/s with $\chi = 1$ or 2. It seems hopeless to measure unambiguously such a difference because the uncertainty of the last precision measurements performed before the 'exactness' assumption had precisely this order of magnitude, namely $\pm 4 \cdot 10^{-9}$ at the 3-sigma level or, equivalently, ± 1.2 m/s.[108]

Therefore, as pointed out in ref.,[94] an experimental test cannot be obtained from the value of the isotropic speed in vacuum but, rather, from its possible *anisotropy*. In fact, with a preferred frame and for $\mathcal{N}_v \neq 1$, an isotropic propagation as in Eq.(53) would only be valid for a special state of motion of the Earth laboratory. This provides the definition of Σ while for a non-zero relative velocity there would be off diagonal elements $g_{0i} \neq 0$ in the effective metric.[105] If Σ exists, we would then expect a light anisotropy $\frac{|\Delta \bar{c}_\theta|}{c} \sim \epsilon_v(v/c)^2 \sim 10^{-15}$, consistently with the presently measured value.

5.2. *Some important technical aspects*

Before considering the experiments, however, a rather technical discussion is necessary for an in-depth comparison with the data. In the mentioned cryogenic experi-
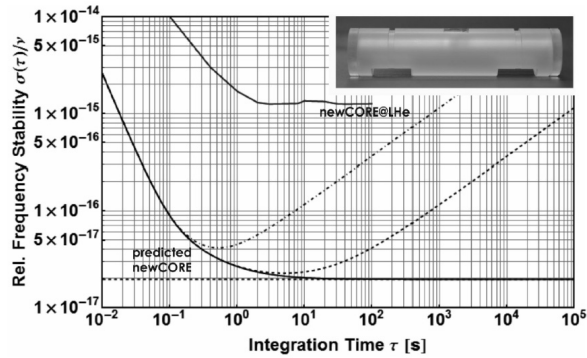
Fig. 21.   *The stability of the fractional frequency shift of ref.[92] at different integration times. The upper solid curve, denoted as 'newCORE', reports the actual measurements with the cryogenic apparatus in 2013. The lower solid, dashed and dot-dashed curves, denoted as 'predicted newCORE', indicate future stability limits $(2 \div 4) \cdot 10^{-17}$ that could be foreseen at that time.*

ment of ref.,[92] the instantaneous signal is not shown explicitly. However, its magnitude can be deduced from its typical variation observed over a characteristic time of 1÷2 seconds, see Fig.21. For a very irregular signal, in fact, this typical variation, of about 10^{-15}, gives the magnitude of the instantaneous signal itself and, indeed, it is in good agreement with the mentioned room-temperature measurements.
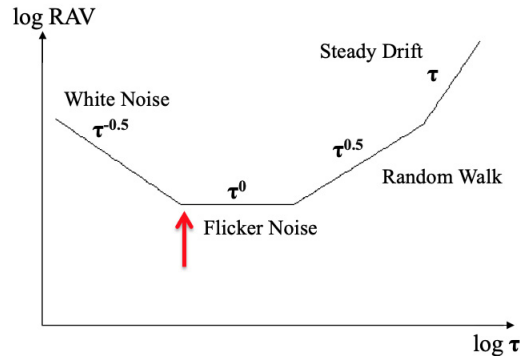

Fig. 22.   *The typical trend of the RAV for a signal in various regimes. The minimum of the white-noise trend $\tau^{-0.5}$ defines the value $\tau = \bar{\tau}$ indicated by the arrow.*

The quantity which is reported in Fig.21 is the Root Square of the Allan Variance (RAV) of the fractional frequency shift. In general, the RAV describes the variation

obtained by sampling a function $f = f(t)$ at steps of time τ. By defining

$$\overline{f}(t_i; \tau) = \frac{1}{\tau} \int_{t_i}^{t_i+\tau} dt\ f(t) \equiv \overline{f}_i \tag{57}$$

one generates a $\tau-$dependent distribution of $\overline{f}_i$ values. In a large time interval $\Lambda = M\tau$, the RAV is then defined as

$$RAV(f, \tau) = \sqrt{RAV^2(f, \tau)} \tag{58}$$

where

$$RAV^2(f, \tau) = \frac{1}{2(M-1)} \sum_{i=1}^{M-1} \left(\overline{f}_i - \overline{f}_{i+1} \right)^2 \tag{59}$$

and the factor of 2 is introduced to obtain the standard variance $\sigma(f)$ for uncorrelated data with zero mean, as for a pure white-noise signal.

Note that the actual measurements in Fig.21 are indicated by the upper solid curve denoted as 'newCORE'. These were obtained with the cryogenic apparatus in 2013 (CORE=Cryogenic Optical REsonators) and were giving a stability at the level of about $1.2 \cdot 10^{-15}$. The lower solid, dashed and dot-dashed curves, denoted as 'predicted newCORE', indicate instead possible improved limits $(2 \div 4) \cdot 10^{-17}$ that could be foreseen at that time. As a matter of fact, these limits have not yet been achieved because the highest stability limits are still larger by an order of magnitude. This persistent signal, which is crucial for our work, does not depend on the absolute temperature and/or the characteristics of the optical cavities.[109]

After this preliminaries, we then arrive at our main point. As anticipated, numerical simulations in our stochastic model indicate that our basic signal has the same characteristics as a universal white noise. This means that it should be compared with the frequency shift of two optical resonators at the largest integration time $\bar{\tau}$ *where the pure white-noise component is as small as possible* but other disturbances, that can affect the measurements, are not yet important, see Fig.22. In the experiments we are presently considering this $\bar{\tau}$ is typically $1 \div 2$ seconds so that one gets the relation with the average magnitude of the instantaneous signal

$$RAV(\Delta\nu, \bar{\tau}) \sim \sigma(\Delta\nu) \sim \langle |\Delta\nu| \rangle_{\text{stat}} \tag{60}$$

5.3. *Comparing our model with experiments in vacuum*

We will now compare with the type of signal observed in[68,90] in vacuum at room temperature. To this end, we will use the relation which connects the frequency shift between two orthogonal resonators $\Delta\nu(\theta; t) = \nu_1(\theta; t) - \nu_2(\theta + \pi/2; t)$ to the angular dependence of the velocity of light, namely see (33)

$$\frac{\Delta\nu(\theta; t)}{\nu_0} = \frac{\Delta\bar{c}_\theta(t)}{c} = 2S(t)\sin 2\theta + 2C(t)\cos 2\theta \tag{61}$$

where $S(t)$ and $C(t)$ are given in Eqs.(34). As in the case of the classical experiments, the velocity components $v_x(t)$ and $v_y(t)$ will be expressed as random Fourier series through the Eqs.(83) and (84) of the Appendix. A simulation of two short-time sequences of $2C(t)$ and $2S(t)$ is shown in Fig.23.
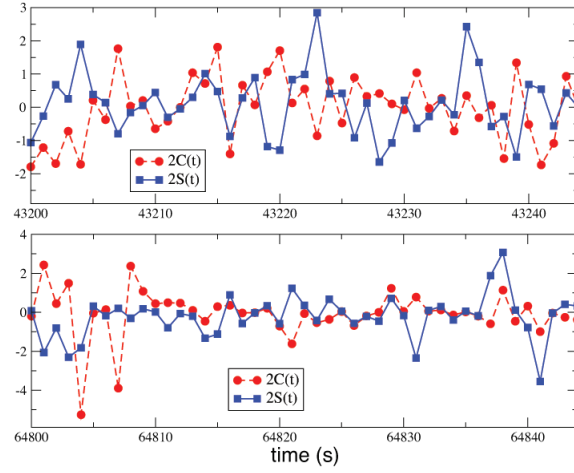

Fig. 23. *For ϵ_v as in Eq.(56) and $\chi = 2$, we report a simulation of two sequence of 45 seconds for the functions $2C(t)$ and $2S(t)$ Eqs.(34). Units are 10^{-15} and the two sets belong to the same random sequence for two sidereal times that differ by 6 hours. The boundaries of the stochastic velocity components, Eqs.(83) and (84) of the Appendix, are controlled by $(V, \alpha, \gamma)_{\mathrm{CMB}}$ through Eqs.(77) and (87). For a laser frequency of $2.8 \cdot 10^{14}$ Hz, the range $\pm 3.5 \cdot 10^{-15}$ corresponds to a typical frequency shift $\Delta \nu$ in the range ± 1 Hz, as in our Fig.19.*

For a quantitative test, we concentrated on the observed value of the RAV of the frequency shift at the end point $\bar{\tau} = 1 \div 2$ seconds of the white-noise branch of the spectrum, see Fig.3, bottom part of[68] . This has a value

$$[RAV(\Delta\nu, \bar{\tau})]_{\mathrm{exp}} = (0.20 \div 0.24) \text{ Hz} \qquad (62)$$

or, in units of the reference frequency $\nu_0 = 2.8 \cdot 10^{14}$ Hz [68]

$$\left[RAV(\frac{\Delta\nu}{\nu_0}, \bar{\tau})\right]_{\mathrm{exp}} = (7.8 \pm 0.7) \cdot 10^{-16} \quad \text{Vacuum} - \text{room temperature} \qquad (63)$$

As anticipated, our instantaneous, stochastic signal for $\Delta\nu(t)$ is, to very good approximation, a pure white noise for which the RAV coincides with the standard variance. At the same time, for a very irregular signal with zero mean of the type shown in Fig. 23, but whose magnitude can have a long-term time dependence, one should replace in Eq. (60) $\langle |\Delta\nu| \rangle_{\mathrm{stat}} \rightarrow \langle |\Delta\nu(t)| \rangle_{\mathrm{stat}}$ and evaluate the RAV in the corresponding temporal range. Therefore, from $\frac{\Delta\nu}{\nu_0} = \frac{\Delta\bar{c}_\theta}{c} \sim \epsilon_v \cdot \frac{v^2}{c^2}$, we arrive at

our prediction

$$\left[RAV(\frac{\Delta\nu(t)}{\nu_0},\bar{\tau})\right]_{\text{theor}} \sim \epsilon_v \, \frac{\langle v_x^2(t) + v_y^2(t)\rangle_{\text{stat}}}{c^2} \sim \frac{\pi^2}{18}\cdot\epsilon_v\cdot\frac{V^2}{c^2}\sin^2 z(t) \qquad (64)$$

Then, by using Eq.(56), for the projection $\tilde{v}(t) = V|\sin z(t)| = 250 \div 370$ Km/s used for the classical experiments, our prediction for the RAV can be expressed as

$$\left[RAV(\frac{\Delta\nu}{\nu_0},\bar{\tau})\right]_{\text{theor}} \sim \frac{\chi}{2}\cdot(8.5\pm 3.5)\cdot 10^{-16} \qquad (65)$$

with $\chi = 1$ or 2. By comparing with the experimental Eq.(63), the data favour $\chi = 2$, which is the only free parameter of our scheme. Also, the good agreement with our theoretical value indicates that, at the end point of the white-noise part of the signal, the corrections to our simplest model should be small.

Notice, however, that the range in Eq.(65) is not a theoretical uncertainty but reflects the daily variations of $V^2\sin^2 z(t)$ in Eq.(64). This means that, depending on the sidereal time, the measurements of the RAV at the white-noise end point $\tau = \bar{\tau}$ should exhibit definite daily variations in the range (for $\chi = 2$)

$$5\cdot 10^{-16} \lesssim \left[RAV(\frac{\Delta\nu}{\nu_0},\bar{\tau})\right]_{\text{theor}} \lesssim 12\cdot 10^{-16} \qquad (66)$$

Thus it becomes crucial to understand whether these variations can be observed.

5.4. *Comparing our model with experiments in solids*

To consider modern experiments in solid dielectrics, we will compare with the very precise work of ref.[70] This is a cryogenic experiment, with microwaves of 12.97 GHz, where almost all electromagnetic energy propagates in a medium, sapphire, with refractive index of about 3 (at microwave frequencies). As anticipated, with a thermal interpretation of the residuals in gaseous media, we expect that the fundamental 10^{-15} vacuum signal considered above, with very precise measurements, should also become visible here. In particular, the large refractivity of the solid $\mathcal{N}_{\text{solid}} - 1 = O(1)$ should play no role.

Following refs.,[8–10] we first observe that for $\mathcal{N}_v = 1 + \epsilon_v$ there is a very tiny difference between the refractive index defined relatively to the ideal vacuum value c and the refractive index relatively to the physical isotropic vacuum value $c/\mathcal{N}_v$ measured on the Earth surface. The relative difference between these two definitions is proportional to $\epsilon_v \lesssim 10^{-9}$ and, for all practical purposes, can be ignored. All materials would now exhibit, however, the same background vacuum anisotropy. To this end, let us replace the average isotropic value

$$\frac{c}{\mathcal{N}_{\text{solid}}} \rightarrow \frac{c}{\mathcal{N}_v\mathcal{N}_{\text{solid}}} \qquad (67)$$

and then use Eq.(18) to replace $\mathcal{N}_v$ in the denominator with its $\theta-$dependent value

$$\bar{\mathcal{N}}_v(\theta) \sim 1 + \epsilon_v\beta^2(1 + \cos^2\theta) \qquad (68)$$

This is equivalent to define a $\theta-$dependent refractive index for the solid dielectric

$$\frac{\bar{\mathcal{N}}_{\text{solid}}(\theta)}{\mathcal{N}_{\text{solid}}} \sim 1 + \epsilon_v \beta^2 (1 + \cos^2 \theta) \tag{69}$$

so that

$$[\bar{c}_\gamma(\theta)]_{\text{solid}} = \frac{c}{\bar{\mathcal{N}}_{\text{solid}}(\theta)} \sim \frac{c}{\mathcal{N}_{\text{solid}}} \left[1 - \epsilon_v \beta^2 (1 + \cos^2 \theta)\right] \tag{70}$$

with an anisotropy

$$\frac{[\Delta \bar{c}_\theta]_{\text{solid}}}{[c/\mathcal{N}_{\text{solid}}]} \sim \epsilon_v \beta^2 \cos 2\theta \sim 10^{-15} \tag{71}$$

In this way, a genuine 10^{-15} vacuum effect, if there, could also be detected in a solid dielectric thus implying the same prediction Eq.(65).
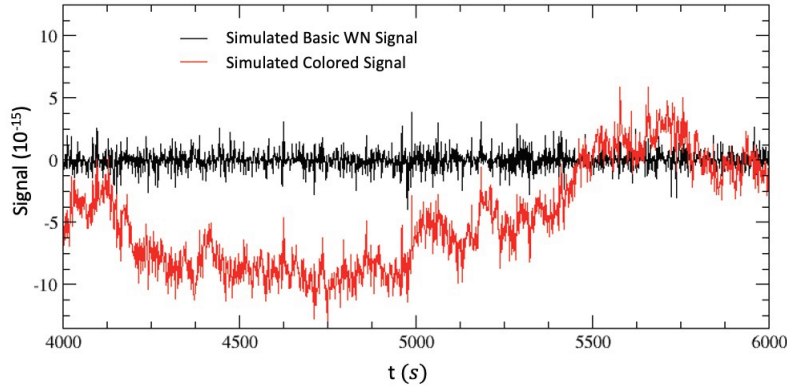

Fig. 24.   *We report two typical sets of 2000 seconds for our basic white-noise (WN) signal and its colored version obtained by Fourier transforming the spectral amplitude of ref.[70] The boundaries of the random velocity components Eqs.(83) and (84) were defined by Eq.(87) by plugging in Eq.(77) the CMB kinematical parameters, for a sidereal time $t = 4000 - 6000$ seconds and for the latitude of Berlin-Duesseldorf, see the Appendix. The figure is taken from ref.[10]*

In ref.,[10] a detailed comparison with[70] was performed. First, from Figure 3(c) of,[70] see also panel b) of our Fig.12, it is seen that the spectral amplitude of this particular apparatus becomes flat at frequencies $\omega \geq 0.5$ Hz indicating that the end-point of the white-noise branch of the signal is at an integration time $\bar{\tau} \sim 1 \div 2$ seconds. The data for the spectral amplitude were then fitted to an analytic, power-law form to describe the lower-frequency part 0.001 Hz $\leq \omega \leq 0.5$ Hz which reflects apparatus-dependent disturbances. This fitted spectrum was then used to generate a signal by Fourier transform. Finally, very long sequences of this signal were stored to produce "colored" version of our basic white-noise signal.

To get a qualitative impression of the effect, we report in Fig.24 a sequence of our basic simulated white-noise signal and a sequence of its colored version. By averaging over many 2000-second sequences of this type, the corresponding RAV's for the two simulated signals are then reported in Fig.25. The experimental RAV extracted from Figure 3(b) of ref.[70] is also reported (for the non-rotating setup). At this stage, the agreement of our simulated, colored signal with the experimental data remains satisfactory only up $\tau = 50$ seconds. Reproducing the signal at larger τ's would have required further efforts but this is not relevant, our scope being just to understand the modifications of our stochastic signal near the endpoint of the white-noise spectrum.
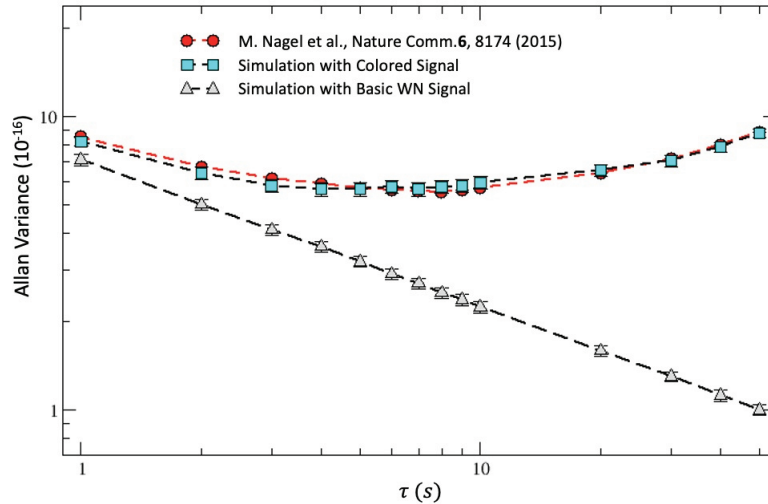

Fig. 25.   *We report the RAV for the fractional frequency shift obtained from many simulations of sequences of 2000 seconds for our basic white-noise (WN) signal (decreasing as $\tau^{-0.5}$) and for its colored version, see Fig.24. The direct experimental results of ref.,[70] for the non-rotating setup, are also shown as red dots. The figure is taken from ref.[10]*

As one can check from Fig.3(b) of ref.,[70] see also the red dots in our Fig.25, the experimental RAV for the fractional frequency shift, at the white-noise end point $\bar{\tau} \sim 1 \div 2$ second, is in the range $(6.8 \div 8.6) \cdot 10^{-16}$, say [70]

$$\left[RAV(\frac{\Delta\nu}{\nu_0}, \bar{\tau}) \right]_{\exp} = (7.7 \pm 0.9) \cdot 10^{-16} \qquad \mathrm{Solid - cryogenic} \qquad (72)$$

As such, it coincides with Eq.(63) that we extracted from ref.[68] after normalizing their experimental result $RAV(\Delta\nu, \bar{\tau})_{\exp} = 0.20 \div 0.24$ Hz to their laser frequency $\nu_0 = 2.8 \cdot 10^{14}$ Hz. At the same time, it is well consistent with our theoretical prediction Eq.(65) for $\chi = 2$. Therefore this beautiful agreement, between ref.[68]

(a vacuum experiment at room temperature) and ref.[70] (a cryogenic experiment in a solid dielectric), on the one hand, and with our theoretical prediction Eq.(65), on the other hand, confirms our interpretation of the data in terms of a stochastic signal associated with the Earth cosmic motion within the CMB and determined by the vacuum refractivity ϵ_v Eq.(56), for $\chi = 2$.

Two ultimate experimental checks still remain. First, as anticipated, one should try to detect our predicted, daily variations Eq.(66). Due to the excellent systematics, these variations should remain visible with both experimental setups. Second, one more complementary test should be performed by placing the vacuum (or solid dielectric) optical cavities on board of a satellite, as in the OPTIS proposal.[110] In this ideal free-fall environment, as in panel (a) of our Fig.20, the typical instantaneous frequency shift should be much smaller (by orders of magnitude) than the corresponding 10^{-15} value measured with the same interferometers on the Earth surface.

6. Summary and outlook

In this paper, we started from the present, basic ambiguity concerning the version of relativity which is *physically realized* in nature, namely Einstein Special Relativity vs. a Lorentzian formulation with a preferred reference frame Σ. This ambiguity is usually presented by a two-step argument. First, the basic quantitative ingredients, namely Lorentz transformations, are the same in both formulations. Second, even in a Lorentzian formulation, Michelson-Morley experiments can only produce null results. Therefore, rather than introducing an experimentally unobservable and logically superfluous entity, it seemed more satisfactory to adopt the point of view of Special Relativity where those effects (length contraction and time dilation), that were at the base of the original Lorentzian formulation, so to speak, become part of the kinematics. In this way, relativity becomes axiomatic and extendable beyond the original domain of the electromagnetic phenomena. This wider perspective has been the main reason for the traditional supremacy given to Einstein's view.

However, discarding all historical aspects, it was emphasized by Bell that a change of perspective, from Special Relativity to a Lorentzian formulation, could be crucial to reconcile hypothetical faster-than-light signals with causality, as with the apparent non-local aspects of the Quantum Theory. In addition, the present view of the lowest-energy state as a Bose condensate of elementary quanta (Higgs particles, quark-antiquark pairs, gluons...), indicates a vacuum structure with some degree of substantiality which could characterize non trivially the form of relativity which is physically realized in nature. So, there may be good reasons for a preferred reference frame but, without the possibility of detecting experimentally an 'ether wind' in laboratory, the difference between the two formulations remains a philosophical problem.

This impossibility-in-principle, however, is somewhat mysterious. While it is certainly true that evidence for both the undulatory and corpuscular aspects of radia-

tion has substantially modified the consideration of an underlying ethereal medium, yet, if Σ exists, only a 'conspiracy' of relativistic effects would make undetectable our motion with respect to it. But this conspiracy works exactly if the velocity of light c_γ propagating in the various interferometers, or more precisely its two-way combination $\bar{c}_\gamma$, coincides with the basic parameter c entering Lorentz transformations. Therefore if $\bar{c}_\gamma \neq c$, as for instance in the presence of matter, where light gets absorbed and then re-emitted, nothing would really prevent an angular dependence $\Delta\bar{c}_\theta = \bar{c}_\gamma(\pi/2 + \theta) - \bar{c}_\gamma(\theta) \neq 0$. If an angular dependence can be detected, and correlated with the cosmic motion of the Earth, the long sought Σ tight to the CMB could finally emerge.

We have thus recalled the two key points of our extensive work. First, one should impose that all measurable effects vanish exactly in the $\bar{c}_\gamma \to c$ limit, i.e. in the *ideal* vacuum limit of a refractive index $\mathcal{N} = 1$. Instead, in the infinitesimal region $\mathcal{N} = 1 + \epsilon$ simple symmetry arguments lead to the relation $\frac{|\Delta\bar{c}_\theta|}{c} \sim \epsilon(v^2/c^2)$. For a typical cosmic $v \sim 300$ km/s and $\epsilon = 2.8 \cdot 10^{-4}$, for air, or $\epsilon = 3.3 \cdot 10^{-5}$, for gaseous helium, this reproduces the order of magnitude of the effects observed in the classical experiments.

The other peculiar aspect of our analysis concerns the observed, irregular character of the data that, giving often substantially different directions of the drift at the same hour on consecutive days, were contradicting the traditional expectation of a regular phenomenon completely determined by the cosmic motion of the Earth. As we have emphasized, here again, there may be a logical gap. The relation between the macroscopic motion of the Earth and the microscopic propagation of light in a laboratory depends on a complicated chain of effects and, ultimately, on the physical nature of the vacuum. By comparing with the motion of a body in a fluid, the standard view corresponds to a form of regular, laminar flow where the projection $\tilde{v}_\mu(t)$ of the global, cosmic velocity, at the site of the experiment, coincides with the local $v_\mu(t)$ that determines the signal in the plane of the interferometer. Instead, some general arguments and some experimental analogies suggest that the *physical vacuum* might rather resemble a turbulent fluid where large-scale and small-scale flows are only related *indirectly*. In this different perspective, with forms of turbulence that, as in most models, become statistically isotropic at small scales, the local $v_\mu(t)$ would fluctuate randomly within boundaries fixed by the global $\tilde{v}_\mu(t)$ (see the Appendix). Therefore, one should analyze the data in phase and amplitude (giving respectively the instantaneous direction and magnitude of the drift) and concentrate on the latter which is positive definite and remains non-zero under any averaging procedure. In this way, by restricting to the amplitudes, experiments always believed in contradiction with each other, as Miller vs. Piccard-Stahel, become consistent, see Fig.9. Most notably, by adopting the parameters $(V, \alpha, \gamma)_{\text{CMB}}$ to fix the boundaries of the local random $v_\mu(t)$ in our stochastic model, one finds a good description of the irregular behaviour of the amplitudes extracted from Joos' very precise observations (see Figs.17 and 18). Viceversa, by fitting Joos' amplitudes with Eqs.(76) and (77), one finds a right ascension $\alpha(\text{fit} - \text{Joos}) = (168 \pm 30)$ de-

grees and an angular declination $\gamma(\text{fit} - \text{Joos}) = (-13 \pm 14)$ degrees which are well consistent with the present values $\alpha(\text{CMB}) \sim 168$ degrees and $\gamma(\text{CMB}) \sim -7$ degrees. The summary of all classical experiments given in Table 3 shows the complete consistency with our theoretical predictions.

To conclude our analysis of the classical experiments in gaseous systems, we have emphasized that our basic relation $\frac{|\Delta \bar{c}_\theta|}{c} \sim \epsilon_{\text{gas}}(v^2/c^2)$ derives from general, symmetry arguments and does *not* explain the ultimate origin of the tiny observed residuals. Due to the consistency with the velocity of 370 km/s, a plausible explanation consists in a collective interaction of gaseous matter with the CMB radiation. This could bring the gas out of equilibrium as if there were an effective temperature difference, $|\Delta T^{\text{gas}}(\theta)| = 0.2 \div 0.3$ mK, in the gas along the two optical paths. This magnitude is slightly smaller than the value of about 1 mK considered by Joos and Shankland and, being just a small fraction of the whole $\Delta T^{\text{CMB}}(\theta) = \pm 3.3$ mK in Eq.(3), indicates the weakness of the collective gas-CMB interactions. Most notably, the thermal interpretation leads to an important prediction. In fact, it implies that if a physical signal could definitely be detected in vacuum then, with very precise measurements, the same signal should also show up in a *solid dielectric* where disturbing temperature differences of a fraction of millikelvin become irrelevant. Detecting such 'non-thermal' light anisotropy, through the combined analysis of the modern experiments in vacuum and in solid dielectrics, for the same cosmic motion indicated by the classical experiments, is thus necessary to confirm the idea of a fundamental preferred frame.

Despite the much higher precision of modern experiments, the assumptions behind the analysis of the data are basically the same as in the classical experiments. A genuine signal is assumed to be a regular phenomenon, depending deterministically on the Earth cosmic motion, so that averaging more and more observations is considered a way of improving the accuracy. But the classical experiments indicate genuine physical fluctuations which are not spurious noise and, instead, express how the cosmic motion of the Earth is actually seen in a detector. Therefore, the present quoted average, namely $\frac{\langle \Delta \bar{c}_\theta \rangle}{c} \lesssim 10^{-18}$, could just reflect the very irregular nature of the signal. Indeed, its typical instantaneous magnitude in vacuum $\frac{|\Delta \bar{c}_\theta|}{c} \sim 10^{-15}$ is about 1000 times larger, see Fig.19 or panel b) of Fig.11.

To understand if this vacuum signal can admit a physical interpretation, a crucial observation is that the same 10^{-15} magnitude is found in measurements where the resonators are made of different materials, in measurements at room-temperature and also in the *cryogenic* regime. Since it is very unlike that spurious effects remain the same in so different conditions, in the same model used for the classical experiments we are driven to the idea of a refractive index $\mathcal{N}_v = 1 + \epsilon_v$ for the vacuum or, more precisely, for the physical vacuum established in an optical cavity placed on the Earth surface. The refractivity ϵ_v should be at the 10^{-9} level, in order to give $\frac{|\Delta \bar{c}_\theta|}{c} \sim \epsilon_v \ (v^2/c^2) \sim 10^{-15}$ and thus would fit with the original idea of ref.[94] The motivation was that, if Einstein's gravity is a phenomenon which emerges, at some

small length scale, from a fundamentally flat space, for an apparatus placed on the Earth surface (which is in free fall with respect to all masses in the Universe but not with respect to the Earth, see Fig.20) there should be a tiny vacuum refractivity $\epsilon_v \sim (2G_N M/c^2 R) \sim 1.39 \cdot 10^{-9}$, where G_N is the Newton constant and M and R are the mass and radius of the Earth. This is the same type of refractivity considered by Eddington, or much more recently by Broekaert, to explain in flat space the deflection of light in a gravitational field. Therefore Michelson-Morley experiments, by detecting a light anisotropy $\frac{|\Delta \bar{c}_\theta|}{c} \sim \epsilon_v \ (v^2/c^2) \ \sim 10^{-15}$, can also resolve this other ambiguity.

With this identification of ϵ_v, we first compared qualitatively the observed signal, in Fig.19 or in panel b) of Fig.11, with simulations in our stochastic model, see Figs.23 and 24. For a more quantitative analysis, we then considered the value of a particular statistical indicator which is used nowadays, namely the Allan Variance of the fractional frequency shift $RAV(\frac{\Delta \nu}{\nu_0}, \tau)$ as function of the integration time τ. Since the irregular signal of our stochastic model has the characteristics of a universal white noise and should represent an irreducible component, we have thus compared with the RAV measured at the *end point* of the white-noise branch of the spectrum. This is defined as the largest integration time $\bar{\tau}$ where the white-noise component is as small as possible but other spurious disturbances, that can affect the measurements, are not yet important, see Fig.22. In this way, for the same velocity range $\tilde{v} = 250 \div 370$ km/s used for the classical experiments, our theoretical prediction Eq.(65) (for $\chi = 2$) is in very good agreement with the results of the most precise experiment in vacuum Eq.(63).

But, then, the second crucial test. As anticipated, if this 10^{-15} signal observed in vacuum has a real physical meaning, the same effect should also be detected with a very precise experiment in a solid dielectric, see Eq.(71). This expectation is confirmed by the extraordinary agreement between Eq.(72) and Eq.(63). Note that the two experiments are completely different because in ref.[70] light propagates in a solid in the cryogenic regime and in ref.[68] light propagates in vacuum at room temperature. As such, there is a plenty of systematic differences. Yet, the two experiments give exactly the same signal *at the white-noise end point*. Therefore, there must be an ubiquitous form of white noise that admits a definite physical interpretation. Our theoretical prediction Eq.(65) is, at present, the only existing explanation. Together with the classical experiments, we thus conclude that there is now an alternative scheme challenging the traditional 'null interpretation' of Michelson-Morley experiments, always presented as a self-evident scientific truth.

We have also discussed two further experimental tests. First, one should try to detect our predicted, daily variations Eq.(66). Second, one should also try to place the optical cavities on a satellite, as in the OPTIS proposal.[110] In this ideal free-fall environment, as in panel (a) of our Fig.20, the typical instantaneous frequency shift should be much smaller (by orders of magnitude) than the corresponding 10^{-15} value measured with the same interferometers on the Earth's surface.

Appendix

In this appendix, we will summarize the stochastic model used in refs.[7–10] to compare with experiments. To make explicit the time dependence of the signal let us first re-write Eq.(19) as

$$\frac{\Delta \bar{c}_\theta(t)}{c} \sim \epsilon \frac{v^2(t)}{c^2} \cos 2(\theta - \theta_2(t)) \tag{73}$$

where $v(t)$ and $\theta_2(t)$ indicate respectively the instantaneous magnitude and direction of the drift in the (x, y) plane of the interferometer. This can also be re-written as

$$\frac{\Delta \bar{c}_\theta(t)}{c} \sim 2S(t) \sin 2\theta + 2C(t) \cos 2\theta \tag{74}$$

with

$$2C(t) = \epsilon \frac{v_x^2(t) - v_y^2(t)}{c^2} \qquad 2S(t) = \epsilon \frac{2v_x(t)v_y(t)}{c^2} \tag{75}$$

and $v_x(t) = v(t)\cos\theta_2(t)$, $v_y(t) = v(t)\sin\theta_2(t)$

As anticipated in Sect.3, the standard assumption to analyze the data has always been based on the idea of regular modulations of the signal associated with a cosmic Earth velocity. In general, this is characterized by a magnitude V, a right ascension α and an angular declination γ. These parameters can be considered constant for short-time observations of a few days where there are no appreciable changes due to the Earth orbital velocity around the sun. In this framework, where the only time dependence is due to the Earth rotation, the traditional identifications are $v(t) \equiv \tilde{v}(t)$ and $\theta_2(t) \equiv \tilde{\theta}_2(t)$ where $\tilde{v}(t)$ and $\tilde{\theta}_2(t)$ derive from the simple application of spherical trigonometry[71]

$$\cos z(t) = \sin\gamma \sin\phi + \cos\gamma \cos\phi \cos(\tau - \alpha) \tag{76}$$

$$\tilde{v}(t) = V \sin z(t) \tag{77}$$

$$\tilde{v}_x(t) = \tilde{v}(t) \cos\tilde{\theta}_2(t) = V [\sin\gamma \cos\phi - \cos\gamma \sin\phi \cos(\tau - \alpha)] \tag{78}$$

$$\tilde{v}_y(t) = \tilde{v}(t) \sin\tilde{\theta}_2(t) = V \cos\gamma \sin(\tau - \alpha) \tag{79}$$

Here $z = z(t)$ is the zenithal distance of $\mathbf{V}$, ϕ is the latitude of the laboratory, $\tau = \omega_{\text{sid}}t$ is the sidereal time of the observation in degrees ($\omega_{\text{sid}} \sim \frac{2\pi}{23^h 56'}$) and the angle θ_2 is counted conventionally from North through East so that North is $\theta_2 = 0$ and East is $\theta_2 = 90^o$. With the identifications $v(t) \equiv \tilde{v}(t)$ and $\theta_2(t) \equiv \tilde{\theta}_2(t)$, one thus arrives to the simple Fourier decomposition

$$S(t) \equiv \tilde{S}(t) = S_0 + S_{s1}\sin\tau + S_{c1}\cos\tau + S_{s2}\sin(2\tau) + S_{c2}\cos(2\tau) \tag{80}$$

$$C(t) \equiv \tilde{C}(t) = C_0 + C_{s1}\sin\tau + C_{c1}\cos\tau + C_{s2}\sin(2\tau) + C_{c2}\cos(2\tau) \tag{81}$$

where the C_k and S_k Fourier coefficients depend on the three parameters (V, α, γ) and are given explicitly in refs.[7,9]

Though, the identification of the instantaneous quantities $v_x(t)$ and $v_y(t)$ with their counterparts $\tilde{v}_x(t)$ and $\tilde{v}_y(t)$ is not necessarily true. As anticipated in Sect.3, one could consider the alternative situation where the velocity field is a non-differentiable function and adopt some other description, for instance a formulation in terms of random Fourier series.[55,72,73] In this other approach, the parameters of the macroscopic motion are used to fix the typical boundaries for a microscopic velocity field which has an intrinsic non-deterministic nature.

The model adopted in refs.[7–10] corresponds to the simplest case of a turbulence which, at small scales, appears homogeneous and isotropic. The analysis can then be embodied in an effective space-time metric for light propagation

$$g^{\mu\nu}(t) \sim \eta^{\mu\nu} + 2\epsilon v^\mu(t)v^\nu(t) \tag{82}$$

where $v^\mu(t)$ is a random 4-velocity field which describes the drift and whose boundaries depend on a smooth field $\tilde{v}^\mu(t)$ determined by the average Earth motion.

For homogeneous turbulence a series representation, suitable for numerical simulations of a discrete signal, can be expressed in the form

$$v_x(t_k) = \sum_{n=1}^\infty [x_n(1)\cos\omega_n t_k + x_n(2)\sin\omega_n t_k] \tag{83}$$

$$v_y(t_k) = \sum_{n=1}^\infty [y_n(1)\cos\omega_n t_k + y_n(2)\sin\omega_n t_k] \tag{84}$$

Here $\omega_n = 2n\pi/T$ and T is the common period of all Fourier components. Furthermore, $t_k = (k-1)\Delta t$, with $k = 1, 2...$, and Δt is the sampling time. Finally, $x_n(i = 1, 2)$ and $y_n(i = 1, 2)$ are random variables with the dimension of a velocity and vanishing mean. In our simulations, the value $T = T_{\text{day}}$= 24 hours and a sampling step $\Delta t = 1$ second were adopted. However, the results would remain unchanged by any rescaling $T \to sT$ and $\Delta t \to s\Delta t$.

In general, we can denote by $[-d_x(t), d_x(t)]$ the range for $x_n(i = 1, 2)$ and by $[-d_y(t), d_y(t)]$ the corresponding range for $y_n(i = 1, 2)$. Statistical isotropy would require to impose $d_x(t) = d_y(t)$. However, to illustrate the more general case, we will first consider $d_x(t) \neq d_y(t)$.

If we assume that the random values of $x_n(i = 1, 2)$ and $y_n(i = 1, 2)$ are chosen with uniform probability, the only non-vanishing (quadratic) statistical averages are

$$\langle x_n^2(i = 1, 2)\rangle_{\text{stat}} = \frac{d_x^2(t)}{3\; n^{2\eta}} \qquad \langle y_n^2(i = 1, 2)\rangle_{\text{stat}} = \frac{d_y^2(t)}{3\; n^{2\eta}} \tag{85}$$

Here, the exponent η ensures finite statistical averages $\langle v_x^2(t)\rangle_{\text{stat}}$ and $\langle v_y^2(t)\rangle_{\text{stat}}$ for an arbitrarily large number of Fourier components. In our simulations, between the two possible alternatives $\eta = 5/6$ and $\eta = 1$ of ref.,[73] we have chosen $\eta = 1$ that corresponds to the Lagrangian picture in which the point where the fluid velocity is measured is a wandering material point in the fluid.

Finally, the connection with the Earth cosmic motion is obtained by identifying $d_x(t) = \tilde{v}_x(t)$ and $d_y(t) = \tilde{v}_y(t)$ as given in Eqs. (76)−(79). If, however, we require statistical isotropy, the relation

$$\tilde{v}_x^2(t) + \tilde{v}_y^2(t) = \tilde{v}^2(t) \tag{86}$$

requires the identification

$$d_x(t) = d_y(t) = \frac{\tilde{v}(t)}{\sqrt{2}} \tag{87}$$

For such isotropic model, by combining Eqs.(83)−(87) and in the limit of an infinite statistics, one gets

$$\langle v_x^2(t)\rangle_{\text{stat}} = \langle v_y^2(t)\rangle_{\text{stat}} = \frac{\tilde{v}^2(t)}{2} \frac{1}{3} \sum_{n=1}^{\infty} \frac{1}{n^2} = \frac{\tilde{v}^2(t)}{2} \frac{\pi^2}{18}$$

$$\langle v_x(t)v_y(t)\rangle_{\text{stat}} = 0 \tag{88}$$

and vanishing statistical averages

$$\langle C(t)\rangle_{\text{stat}} = 0 \qquad\qquad \langle S(t)\rangle_{\text{stat}} = 0 \tag{89}$$

at *any* time t, see Eqs.(75). Therefore, by construction, this model gives a definite non-zero signal but, if the same signal were fitted with Eqs.(80) and (81), it would also give average values $(C_k)^{\text{avg}} = 0$, $(S_k)^{\text{avg}} = 0$ for the Fourier coefficients.

To understand how radical is the modification produced by Eqs.(89), we recall the traditional procedure adopted in the classical experiments. One was measuring the fringe shifts at some given sidereal time on consecutive days so that changes of the orbital velocity were negligible. Then, see Eqs.(20) and (74), the measured shifts at the various angle θ were averaged

$$\langle\frac{\Delta\lambda(\theta;t)}{\lambda}\rangle_{\text{stat}} = \frac{2D}{\lambda}\left[2\sin 2\theta \langle S(t)\rangle_{\text{stat}} + 2\cos 2\theta \langle C(t)\rangle_{\text{stat}}\right] \tag{90}$$

and finally these average values were compared with models for the Earth cosmic motion.

However if the signal is so irregular that, by increasing the number of measurements, $\langle C(t)\rangle_{\text{stat}} \to 0$ and $\langle S(t)\rangle_{\text{stat}} \to 0$ the averages Eq.(90) would have no meaning. In fact, these averages would be non vanishing just because the statistics is finite. In particular, the direction $\theta_2(t)$ of the drift (defined by the relation $\tan 2\theta_2(t) = S(t)/C(t)$) would vary randomly with no definite limit.

This is why one should concentrate the analysis on the 2nd-harmonic amplitudes

$$A_2(t) = \frac{2D}{\lambda} 2\sqrt{S^2(t) + C^2(t)} \sim \frac{2D}{\lambda} \epsilon\frac{v_x^2(t) + v_y^2(t)}{c^2} \tag{91}$$

which are positive-definite and remain non-zero under the averaging procedure. Moreover, these are rotational-invariant quantities and their statistical average

$$\langle A_2(t)\rangle_{\text{stat}} \sim \frac{2D}{\lambda} \cdot \frac{\pi^2}{18} \cdot \epsilon \cdot \frac{V^2 \sin^2 z(t)}{c^2} \tag{92}$$

would remain unchanged in the isotropic model Eq.(87) or with the alternative choice $d_x(t) \equiv \tilde{v}_x(t)$ and $d_y(t) \equiv \tilde{v}_y(t)$. Analogous considerations hold for the modern experiments where $\frac{\Delta \bar{c}_\theta(t)}{c}$ is extracted from the frequency shift of two optical resonators. Again, the $C(t)$ and $S(t)$ obtained, through Eq.(74), from the very irregular, measured signal (see e.g. Fig.19), are compared with the slowly varying parameterizations Eqs.(80) and (81) to extract the C_k and S_k Fourier coefficients. Then, by comparing with our simulation of the $C(t)$ and $S(t)$ in Fig.23, it is no surprise if the average values $(C_k)^{\text{avg}} \to 0$, $(S_k)^{\text{avg}} \to 0$ by simply increasing the number of observations.

References

1. A. Einstein, *Zur Elektrodynamik bewegter Körper*, Ann. der Physik, 17 (1905) 891;(English translation in: The Principle of Relativity by H. A. Lorentz et al., Methuen 1923)

2. H. A. Lorentz, *Electromagnetic phenomena in a system moving with any velocity smaller than that of light*, Proc. Acad. of Sci. Amsterdam, **6** 1904.

3. A. Ungar,*The relativistic composite-velocity reciprocity principle*, Found. of Phys. **30**, 331 (2000).

4. J. P. Costella, B. H. J. McKellar, A. A. Rawlinson, G. J. Stephenson Jr, *The Thomas rotation*, Am. J. Phys. **69**, 837 (2001).

5. K. O' Donnell and M. Visser,*Elementary analysis of the special relativistic combination of velocities, Wigner rotation, and Thomas precession*, Eur. J. Phys. **32**, 1033 (2011).

6. Full reference to all papers by J. S. Bell, can be found in the Volume Collection, *Speakable and Unspeakable in Quantum Mechanics*, 2nd edition, Cambridge University Press, 2004.

7. M. Consoli, C. Matheson and A. Pluchino, *The classical ether-drift experiments: a modern re-interpretation* Eur. Phys. J. Plus, **128** (2013) 71.

8. M. Consoli and A. Pluchino, *Cosmic Microwave Background and the issue of a fundamental preferred frame*, Eur. Phys. Jour. Plus **133** (2018) 295.

9. M. Consoli and A. Pluchino, *Michelson-Morley Experiments: an Enigma for Physics and the History of Science*, World Scientific 2019, ISBN 978-981-3278-18-9.

10. M. Consoli and A. Pluchino, *CMB, preferred reference system and dragging of light in the Earth's frame*, Universe **7** (2021) 311;arXiv:2109.03047 [physics.gen-ph].

11. T. Maudlin, *Quantum Non-Locality and Relativity*, Blackwell, Cambridge, 2011.

12. N. Gisin, *Quantum Chance*, Springer Int. Publ. 2014.

13. J. Bricmont, *Making Sense of Quantum Mechanics*, Springer Int. Publ. 2016.

14. A. Einstein, B. Podolski and N. Rosen, *Can quantum-mechanical description of physical reality be considered complete?*, Phys. Rev.**47** (1935) 777.

15. D. Salart, A. Baas, C. Branciard, N. Gisin and H. Zbinden, *Testing spooky action at a distance*, Nature **454** (2008) 861.

16. J.-D. Bancal, S. Pironio, A. Acin, Y.-C. Liang, V. Scarani, and N. Gisin, *Quantum nonlocality based on finite-speed causal influences leads to superluminal signaling*, Nature Physics **8** (2012) 867.

17. P. A. M. Dirac, *Development of the Physicist's Conception of Nature*, in The Physicist's Conception of Nature, J. Mehra Ed., Reidel, Boston 1973.

18. A. Aspect, J. Dalibard, G. Roger, *Experimental test of Bell's inequalities using time-varying analyzers*, Phys. Rev. Lett. **49**, 1804 (1982).

19. J. F. Clauser, *Experimental investigation of a polarization correlation anomaly*, Phys. Rev. Lett. **36**, 1223 (1976).

20. G. Weihs, T. Jennewein, C. Simon, H. Weinfurter, and A. Zeilinger, *Violation of Bell's Inequality under Strict Einstein Locality Conditions*, Phys. Rev. Lett. **81**, 5039 (1998)

21. A. Aspect, *Speech at the Nobel Prize banquet*, December 2022.

22. M. Consoli and E. Costanzo, *Is the physical vacuum a preferred frame?*, Eur. Phys. Journ. **C54** (2008) 285.

23. M. Consoli and E. Costanzo, *Precision tests with a new class of dedicated ether-drift experiments*, Eur. Phys. Journ. **C55** (2008) 469.

24. M. Consoli, *Probing the vacuum of particle physics with precise laser interferometry*, Found. of Phys. **45**, 22 (2015).

25. M. Consoli, A. Pluchino, P. Zizzi, *Quantum Non-Locality and the CMB: what Experiments say*, Universe **8** (2022) 48; arXiv:2209.06858 [physics.gen-ph].

26. R. Y. Chiao, *Conceptual tensions between quantum mechanics and general relativity: Are there experimental consequences?*, in "Science and Ultimate Reality: From Quantum to Cosmos", honoring John Wheeler's 90th birthday. J. D. Barrow, P. C. W. Davies, and C. L. Harper eds. Cambridge University Press (2003); arXiv:gr-qc/0303100.

27. G. 't Hooft, *In Search of the Ultimate Building Blocks*, Cambridge Univ. Press 1997, p.70.

28. See, for instance, R. F. Streater and A. S. Wightman, *PCT, Spin and Statistics, and all that*, W. A. Benjamin, New York 1964.

29. I.E. Segal, *Is the Physical Vacuum Really Lorentz-Invariant?*, in Differential Geometry, Group Representations, and Quantization, J.D. Hennig, W.Lücke, J. Tolar, Eds. Lecture Notes in Physics Vol. 379, Springer 1991.

30. M. Yoon and D. Huterer, *Kinematic Dipole Detection With Galaxy Surveys: Forecasts And Requirements*, Astrophys. J. Lett. **813** (2015) L18.

31. G. F. Smoot, *Cosmic microwave background radiation anisotropies: Their discovery and utilization*, Nobel Lecture, Rev. Mod. Phys. **79**, 1349 (2007).

32. L. Hardy, *Quantum mechanics, local realistic theories, and Lorentz-invariant realistic theories*, Phys. Rev. Lett. **68** (1992) 2981.

33. A. A. Michelson and E. W. Morley, *On the Relative Motion of the Earth and the*

Luminiferous Ether, Am. J. Sci. **34**, 333 (1887).

34. E. W. Morley and D. C. Miller, Phil. Mag. **9** (1905) 680.

35. D. C. Miller, *The Ether-Drift Experiment and the Determination of the Absolute Motion of the Earth*, Rev. Mod. Phys. **5**, 203 (1933).

36. A. A. Michelson, et al., *Conference on the Ether-Drift Experiments*, Ap. J. **68** (1928) p. 341-402.

37. K. K. Illingworth, *A Repetition of the Michelson-Morley Experiment Using Kennedy's Refinement*, Phys. Rev. **30**, 692 (1927).

38. R. Tomaschek, *About the Michelson experiment with fixed star light*, Astron. Nachrichten, **219**, 301 (1923), English translation.

39. A. Piccard and E. Stahel, *REALIZATION OF THE EXPERIMENT OF MICHELSON IN BALLOON AND ON DRY LAND*, Journ. de Physique et Le Radium **IX** (1928) No.2.

40. A. A. Michelson, F. G. Pease and F. Pearson,*Repetition of the Michelson-Morley Experiment*, Nature, **123**, 88 (1929).

41. A. A. Michelson, F. G. Pease and F. Pearson, *Repetition of the Michelson-Morley experiment*, J. Opt. Soc. Am. **18**, 181 (1929).

42. F. G. Pease, *Ether-Drift Data*, Publ. of the Astr. Soc. of the Pacific, **XLII**, 197 (1930).

43. G. Joos, *Die Jenaer Wiederholung des Michelsonversuchs*, Ann. d. Physik **7**, 385 (1930).

44. H. Müller, S. Herrmann, C. Braxmaier, S. Schiller, A. Peters, *Precision test of the isotropy of light propagation*, Appl. Phys. B **77**, 719 (2003).

45. H. A. Lorentz, *The Theory of Electrons*, Leipzig 1909, B. G. Teubner Editor.

46. J. M. Jauch and K. M. Watson, *Phenomenological Quantum-Electrodynamics*, Phys. Rev. **74**, 950 (1948).

47. R. J. Kennedy,*Simplified theory of the Michelson-Morley experiment*, Phys. Rev. **47**, 965 (1935).

48. J. C. Maxwell, *Ether*, Encyclopaedia Britannica, 9th Edition, 1878.

49. M. Born, *Einstein's Theory of Relativity*, Dover Publ., New York, 1962.

50. M. Consoli and E. Costanzo, *Old and new ether-drift experiments: A sharp test for a preferred frame*, N. Cimento B **119**, 393 (2004).

51. W. M. Hicks, *On the Michelson-Morley experiment relating to the drift of the aether*, Phil. Mag. **3**, 9 (1902).

52. M. Consoli, A. Pluchino and A. Rapisarda,*Basic randomness of nature and ether-drift experiments*, Chaos, Solitons and Fractals **44**, 1089 (2011).

53. M. Consoli, A. Pluchino, A. Rapisarda and S. Tudisco, *The vacuum as a form of turbulent fluid: motivations, experiments, implications*, Physica **A394**, 61 (2014).

54. R. P. Feynman, R. B. Leighton and M. Sands, *The Feynman Lectures on Physics*, Addison Wesley Publ. Co. 1963.

55. L. Onsager, N. Cimento, *Statistical hydrodynamics*, Suppl. **6**, 279 (1949).

56. G. L. Eyink and K. R. Sreenivasan, *Onsager and the theory of hydrodynamic turbulence*, Rev. Mod. Phys. **78**, 87 (2006).

57. E. T. Whittaker,*A History of the Theories of Aether and Electricity*, Dover Publ., New York 1989.

58. P. A. M. Dirac, *Is there an Aether?*, Nature **168**, 906 (1951).

59. O. V. Troshkin, *On wave properties of an incompressible turbulent fluid*, Physica A **168** (1990) 881.

60. H. E. Puthoff,*Linearized turbulent flow as an analog model for linearized General Relativity*, arXiv:0808.3401 [physics.gen-ph].

61. T. D. Tsankov,*Classical Electrodynamics and the Turbulent Aether Hypothesis*, Preprint February 2009, unpublished.

62. L. A. Saul, *Spin Waves as Metric in a Kinetic Space-Time*, Phys. Lett. **A 314** (2003) 472.

63. M. Consoli, *A kinetic basis for space-time symmetries*, Phys. Lett. **A376** (2012) 3377.

64. E. Nelson, *A derivation of the Schrödinger Equation from Newtonian Mechanics*, Phys. Rev. **150** (1966) 1079.

65. P. Jizba and H. Kleinert, *Superstatistics approach to path integral for a relativistic particle* Phys. Rev. D **82** (2010) 085016.

66. P. Jizba, F. Scardigli, *Special Relativity induced by Granular Space*, Eur. Phys. J. C**73** (2013) 2491.

67. U. Frisch, *Turbulence The Legacy of A. N. Kolmogorov*, Cambridge University Press, 1995.

68. Q. Chen, E. Magoulakis, and S. Schiller,*High-sensitivity crossed-resonator laser apparatus for improved tests of Lorentz invariance and of space-time fluctuations*, Phys. Rev. D **93** , 022003 (2016).

69. S. Rizzo, A. Rapisarda, *Environmental Atmospheric Turbulence at Florence Airport*, arXiv:cond-mat/0406684 [cond-mat.stat-mech].

70. M. Nagel, S. R. Parker, E. V. Kovalchuk, P. L. Stanwix, J. G. Hartnett, E. N. Ivanov, A. Peters, M. E. Tobar, *Direct terrestrial test of Lorentz symmetry in electrodynamics to* 10^{-18}, Nature Comm.**6**, 8174 (2015).

71. J. J. Nassau and P. M. Morse,*A Study of Solar Motion by Harmonic Analysis*, Ap. J. **65**, 73 (1927).

72. L. D. Landau and E. M. Lifshitz,*Fluid Mechanics*, Pergamon Press 1959.

73. J. C. H. Fung et al., *Kinematic simulation of homogeneous turbulence by unsteady random Fourier modes*, J. Fluid Mech. **236**, 281 (1992).

74. R. S. Shankland, S. W. McCuskey, F. C. Leone, G. Kuerti, *New Analysis of the Interferometer Observations of Dayton C. Miller*, Rev. Mod. Phys.**27**, 167 (1955).

75. D. C. Miller, *Comments on Dr. Georg Joos's Criticism of the Ether-Drift Experiment*,

Phys. Rev. **45** (1934) 114.

76. L. S. Swenson Jr., *The Ethereal Aether, A History of the Michelson-Morley-Miller Aether-Drift Experiments*, 1880-1930. University of Texas Press, Austin 1972.

77. Loyd S. Swenson Jr., *The Michelson-Morley-Miller Experiments before and after 1905*, Journ. for the History of Astronomy, **1**, 56 (1970).

78. J. Shamir and R. Fox, *A New Experimental Test of Special Relativity*, N. Cim. **62B**, 258 (1969).

79. M. Consoli, A. Pluchino and A. Rapisarda, *Cosmic Background Radiation and 'ether-drift' experiments*, Europhysics Lett. **113**, 19001 (2016).

80. G. Joos, *Note on the Repetition of the Michelson-Morley Experiment*, Phys. Rev. **45**, 114 (1934).

81. E. R. Farkas and W. W. Webb, *Precise and millidegree stable control for fluorescense imaging*, Rev. Scient. Instr. **81**, 093704 (2010).

82. Y. Zhao, D. L. Trumper, R. K. Heilmann, M. L. Schattenburg, *Optimizatiom and temperature mapping of an ultra-high thermal stability enviromental enclosure*, Precision Engin. **34**, 164 (2010).

83. I. P. Prikhodko, A. A. Trusov, A. M. Shkel, *Compensation of drifts in high-Q MEMS gyroscopes using temperature self-sensing*, Sensors and Actuators A **201**, 517 (2013).

84. S. W. W. Manley, *A novel Michelson-Morley experiment testing for anisotropic light propagation in gas without violation of local Lorentz invariance*, Eur. Phys. J. Plus **138**, 206 (2023).

85. R. V. Pound, *Electronic frequency stabilization of microwave oscillators*, Rev. Sci. Instr. **17**, 490 (1946).

86. R. W. P. Drever, J. L. Hall, F. V. Kowalski, J. Hough, G. M. Ford, A. J. Munley, H. Ward, *Laser phase and frequency stabilization using an optical resonator*, Appl. Phys. B **31**, 97 (1983).

87. E. D. Black, *An introduction to Pound-Drever-Hall laser frequency stabilization*, Am. J. Phys. **69**, 79 (2001).

88. A. Brillet and J. L. Hall, *Improved Laser Test of the Isotropy of Space*, Phys. Rev. Lett. **42**, 549 (1979).

89. G. F. Smoot, M. V. Gorenstein, and R. A. Muller, *Detection of Anisotropy in the Cosmic Blackbody Radiation*, Phys. Rev. Lett. **39**, 898 (1977).

90. Ch. Eisele, M. Okhapin, A. Nevsky, S. Schiller, *A crossed optical cavities apparatus for a precision test of the isotropy of light propagation*, Opt. Comm. **281**, 1189 (2008).

91. S. Herrmann, A. Senger, K. Möhle, M. Nagel, E. V. Kovalchuk, A. Peters, *Rotating optical cavity experiment testing Lorentz invariance at the 10^{-17} level*, Phys.Rev. D **80**, 10511 (2009).

92. M. Nagel, K. Möhle, K. Döringshoff, S. Schikora, E.V. Kovalchuk, A. Peters, *Ultra-stable Cryogenic Optical Resonators For Tests Of Fundamental Physics*,

arXiv:1308.5582[physics.optics].

93. K. Numata, A, Kemery and J. Camp, *Thermal-Noise Limit in the Frequency Stabilization of Lasers with Rigid Cavities*, Phys. Rev. Lett. **93**, 250602 (2004).

94. M. Consoli and L. Pappalardo, *Emergent gravity and ether-drift experiments*, Gen. Rel. and Grav. **42**, 2585 (2010).

95. C. Barcelo, S. Liberati and M. Visser, *Analog gravity from Bose-Einstein condensates*, Class. Quantum Grav. **18**, 3595 (2001).

96. M. Visser, C. Barcelo and S. Liberati, *Analogue models of and for gravity*, Gen. Rel. Grav. **34**, 1719 (2002).

97. G. E. Volovik, *Superfluid analogies of cosmological phenomena*, Phys. Rep. **351**, 195 (2001).

98. H. Yilmaz, *New Approach to General Relativity*, Phys. Rev. **111**, 1417 (1958).

99. R. P. Feynman, in *Superstrings: A Theory of Everything?* , P. C. W. Davies and J. Brown Eds., Cambridge University Press, 1997, pag. 201.

100. E. G. Adelberger, *New tests of Einstein's equivalence principle and Newton's inverse-square law*, Class. Quantum Grav. **18**, 2397 (2001).

101. R. D'E. Atkinson, *General relativity in Euclidean terms* Proc. R. Soc. **272**, 60 (1963).

102. K. Thorne, *Black Holes and Time Warps: Einstein's Outrageous Legacy*, W. W. Norton and Co. Inc, New York and London, 1994, see Chapt. 11 "What is Reality?".

103. R. J. Cook, *Physical time and physical space in general relativity*, Am. J. Phys. **72**, 214 (2004).

104. A. S. Eddington, *Space, Time and Gravitation*, Cambridge University Press, 1920.

105. A. M. Volkov, A. A. Izmest'ev, and G. V. Skrotski, *The propagation of electromagnetic waves in a riemannian space*, Sov. Phys. JETP **32**, 686 (1971).

106. J. Broekaert, *A Spatially-VSL Gravity Model with 1-PN limit of GRT*, Found. of Phys. **38**, 409 (2008).

107. L. D. Landau and E. M. Lifshitz, *The Classical Theory of Fields*, Pergamon Press, 1971, p.257.

108. D. A. Jennings, R. E. Drullinger, K. M. Evenson, C. R. Pollock, J. S. Wells, *The Continuity of the Meter: The Redefinition of the Meter and the Speed of Visible Light*, Journ. of Res. Nat. Bur. Stand. **92**, 11 (1987).

109. M. Nagel, *Design of a next-generation modern Michelson-Morley experiment*, PhD Thesis, (Humboldt U., Berlin), March 2022.

110. C. Lämmerzahl et al., *OPTIS: a satellite-based test of special and general relativity*, Class. Quantum Gravity **18**, 2499 (2001).